JOURNAL OF MORPHOLOGY 267:70–102 (2006)

Cranial Anatomy of the Spade-Headed Amphisbaenian *Diplometopon zarudnyi* (Squamata, Amphisbaenia) Based on High-Resolution X-ray Computed Tomography

Jessica Anderson Maisano,[1]* Maureen Kearney,[2] and Timothy Rowe[1]

[1]*Jackson School of Geosciences, The University of Texas at Austin, Austin, Texas 78712*
[2]*Department of Zoology, Field Museum of Natural History, Chicago, Illinois 60605*

ABSTRACT The skull of the trogonophid amphisbaenian *Diplometopon zarudnyi* is described from high-resolution X-ray computed tomographic (HRXCT) imagery of a whole museum specimen preserved in ETOH. The skull was digitally resliced and disarticulated into individual elements, producing novel visualizations that allow detailed morphological analysis of its three-dimensionally complex structure. The prefrontal and jugal are absent in *Diplometopon*. The septomaxilla is present but hidden entirely from superficial view. In contrast to previous studies, we recognize a splenial fused to the compound bone of the mandible and a squamosal fused to the otic–occipital complex. Comparison of *Diplometopon* to the two other amphisbaenians previously described in comparable detail, *Rhineura hatcherii* and *Amphisbaena alba*, reveals a mosaic of cranial similarities and differences. Both *Diplometopon* and *Rhineura* exhibit a craniofacial angulation and expanded rostral blade related to use of the head as a digging tool, but the detailed architecture of these features is quite different. Additionally, whereas the snout of *Rhineura* exhibits a high degree of sculpturing and sensory innervation, this is not the case in *Diplometopon*. Unlike in *Rhineura* and *Amphisbaena*, the cranial elements of *Diplometopon* do not exhibit an extensive degree of overlap or complex interlocking sutures; instead, most of the cranial elements lie in loose apposition to each other. The degree to which this mosaic of features reflects functional demands, shared ancestry, and/or convergence is unclear in the absence of a stable hypothesis of amphisbaenian phylogeny. J. Morphol. 267:70–102, 2006.

KEY WORDS: Squamata; Amphisbaenia; Trogonophidae; *Diplometopon zarudnyi*; cranial anatomy; computed tomography

Amphisbaenians ("worm lizards") are a poorly known group of fossorial squamate reptiles, nearly all of which are limbless. Their secretive habits in the wild make them difficult to collect and, as a result, museum specimens generally are rare and too precious for traditional, destructive anatomical studies. Worm lizards exhibit dramatic cranial modifications related to their head-first burrowing behavior in the soils they inhabit. Four basic cranial morphotypes ("shovel-headed," "round-headed," "keel-headed," and "spade-headed") are recognized (Gans, 1974), and the monophyly of these morphotypes is the subject of renewed study from a phylogenetic perspective (Kearney, 2003). A recent molecular study (Kearney and Stuart, 2004) suggests that some amphisbaenian cranial morphotypes may have evolved convergently among geographically distinct, independent lineages, providing the impetus to examine the skull anatomy of these forms in more detail.

A bone-by-bone study of the "round-headed" amphisbaenid, *Amphisbaena alba*, was conducted by Montero and Gans (1999). Kearney et al. (2005) provided the first detailed cranial description of an amphisbaenian based on high-resolution X-ray computed tomographic (HRXCT) data. The description of that species, *Rhineura hatcherii*, revealed numerous new details of skull construction in a "shovel-headed" rhineurid. The purpose of the present study is to build on these works, providing a detailed cranial description of the "spade-headed" morphotype seen in trogonophids. The use of nondestructive HRXCT techniques is especially well suited to amphisbaenians due to the three-dimensional complexity of their skulls. Ultimately, we aim to compare and contrast all four amphisbaenian cranial morphotypes using HRXCT to assess the evolutionary modifications of each cranial shape/digging mode, and to fill in knowledge gaps in amphisbaenian cranial anatomy relative to other squamates.

Diplometopon zarudnyi (hereafter *Diplometopon*) is monospecific and occurs in arid habitats in western Iran, southern Iraq, Kuwait, Oman, and northern Saudi Arabia (Gans, 1978). It inhabits aeolian sand deposits, but is known to emerge onto the sur-

Contract grant sponsor: National Science Foundation (NSF); Contract grant numbers: EF-0334961 (to M.K.); IIS-0208675 (to T.R.).

*Correspondence to: Jessica Maisano, Jackson School of Geosciences, The University of Texas at Austin, Austin, TX 78712.
E-mail: maisano@mail.utexas.edu

Published online 28 October 2005 in
Wiley InterScience (www.interscience.wiley.com)
DOI: 10.1002/jmor.10388

face to breed. All trogonophids use a stereotyped, oscillating burrowing behavior in which the head is rotated about the long axis of the body in one direction, then reversed to the other direction, thereby loosening soil from the end of the tunnel (Gans, 1974). Trogonophid monophyly is well corroborated by several synapomorphies, including a strong craniofacial angulation, a highly modified pectoral girdle, acrodont dentition, and a short tail:body ratio (Gans, 1960; Kearney, 2003).

The cranial anatomy of *Diplometopon* has been described by Gans (1960), and in somewhat more detail by El-Assy and Al-Nassar (1976), using classical techniques. We use HRXCT data to describe the skull in a comprehensive bone-by-bone approach, to provide both a thorough cranial description of a trogonophid amphisbaenian and a general morphological characterization of the "spade-headed" morphotype. We offer preliminary comparisons with *Rhineura hatcherii* (hereafter *Rhineura*) and *Amphisbaena alba* (hereafter *Amphisbaena*), the only other amphisbaenians currently known in comparable detail. We also present additional character data for comparison among amphisbaenians generally, with the hope that these will contribute toward greater resolution of amphisbaenian phylogeny in future studies.

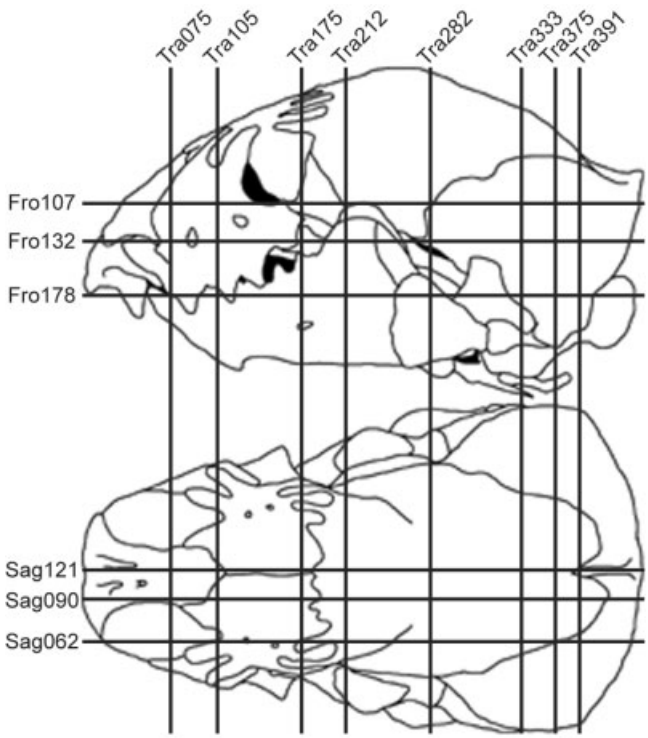

Fig. 1. *Diplometopon zarudnyi* (FMNH 64429). Diagram showing approximate relative positions and orientations of labeled HRXCT slices shown in Figures 2–4.

MATERIALS AND METHODS

This description is based primarily on a single HRXCT-scanned specimen of *Diplometopon* (Field Museum of Natural History, FMNH 64429) collected from Qatif Oasis, Saudi Arabia. While studying this primary specimen, we also compared it to skeletal specimens (FMNH 206115, 74007) and a cleared-and-stained preparation (National Museum of Natural History, USNM 141833). Given the level of detail of the following description, and the availability of HRXCT data for only one specimen, some aspects of the internal structure of the skull may be subject to individual variation not recognized here.

The specimen was scanned at the High-Resolution X-ray CT Facility at The University of Texas at Austin using the following parameters. A FeinFocus microfocal X-ray source operating at 180 kV and 0.133 mA with no X-ray prefilter was employed. An empty container wedge was used. Slice thickness corresponded to 2 lines in a CCD image intensifier imaging system, with a source-to-object distance of 41 mm. For each slice, 1,000 views were taken with five samples per view. The field of image reconstruction was 9.5 mm and an image reconstruction offset of 6,200 was used with a reconstruction scale of 1,600.

The dataset consists of 459 HRXCT slices taken along an oblique axis of the skull from the tip of the snout to the occiput. The scan axis was offset ~20° from orthogonal due to a stiff tilt of the specimen's head relative to its body. Each slice image was gathered at 1024 × 1024 pixels resolution, resulting in an in-plane resolution of 9 μm per pixel. Each slice represents a thickness and spacing of 192 μm, resulting in no overlap between slices. The dataset was digitally resliced along the true orthogonal axes of the skull—transverse (=coronal, front to back), frontal (=horizontal, top to bottom), and sagittal (left to right)—using VoxBlast® (Vaytek, Fairfield, IA). Figure 1 illustrates the relative position of the labeled HRXCT slices shown in Figures 2–4. All references to particular slice numbers refer to the orthogonally resliced dataset, not the original scan dataset.

Individual elements of the skull were digitally isolated by hand by tracing sutures (which are readily apparent) in the original scan images using Adobe PhotoShop® (San Jose, CA), then rendered in three dimensions using VGStudio MAX® 1.2 (Volume Graphics, Heidelberg, Germany). All elements were rotated to the true orthogonal axes of the skull prior to rendering. For paired elements, the left element was isolated except in the case of the mandible, where sutures were more distinct on the right side. Right mandibular elements were mirrored to maintain consistency in spatial orientation in the figures. The cranial bones and mandible are described separately.

The skull as a whole (Fig. 5) is described first, followed by each individual element (Figs. 6–25). The HRXCT slices spanned by each element are noted at the beginning of the description of that element, and selected labeled HRXCT slices (Figs. 1–4) illustrate the internal anatomy of the skull in transverse (Tra), frontal (Fro), and sagittal (Sag) slice planes. Slice numbers are referenced throughout the description.

An interactive, web-deliverable version of the HRXCT dataset keyed to the slice numbers cited below, as well as animations of all isolated bones, can be viewed at http://www.digimorph.org/specimens/Diplometopon_zarudnyi, and the original full-resolution HRXCT data are available from the authors.

RESULTS

Overview of Skull (Fig. 5)

The skull of *Diplometopon* is short and broad in comparison to the elongated skulls seen in many amphisbaenians. It measures 8.2 mm from the tip of the snout to the posterior tip of the occipital condyle, and 4.8 mm at its widest expanse, at the level of the external opening of the jugular recess. The skull displays the typical trogonophid condition (Kearney, 2003), in which the spatulate snout projects sharply

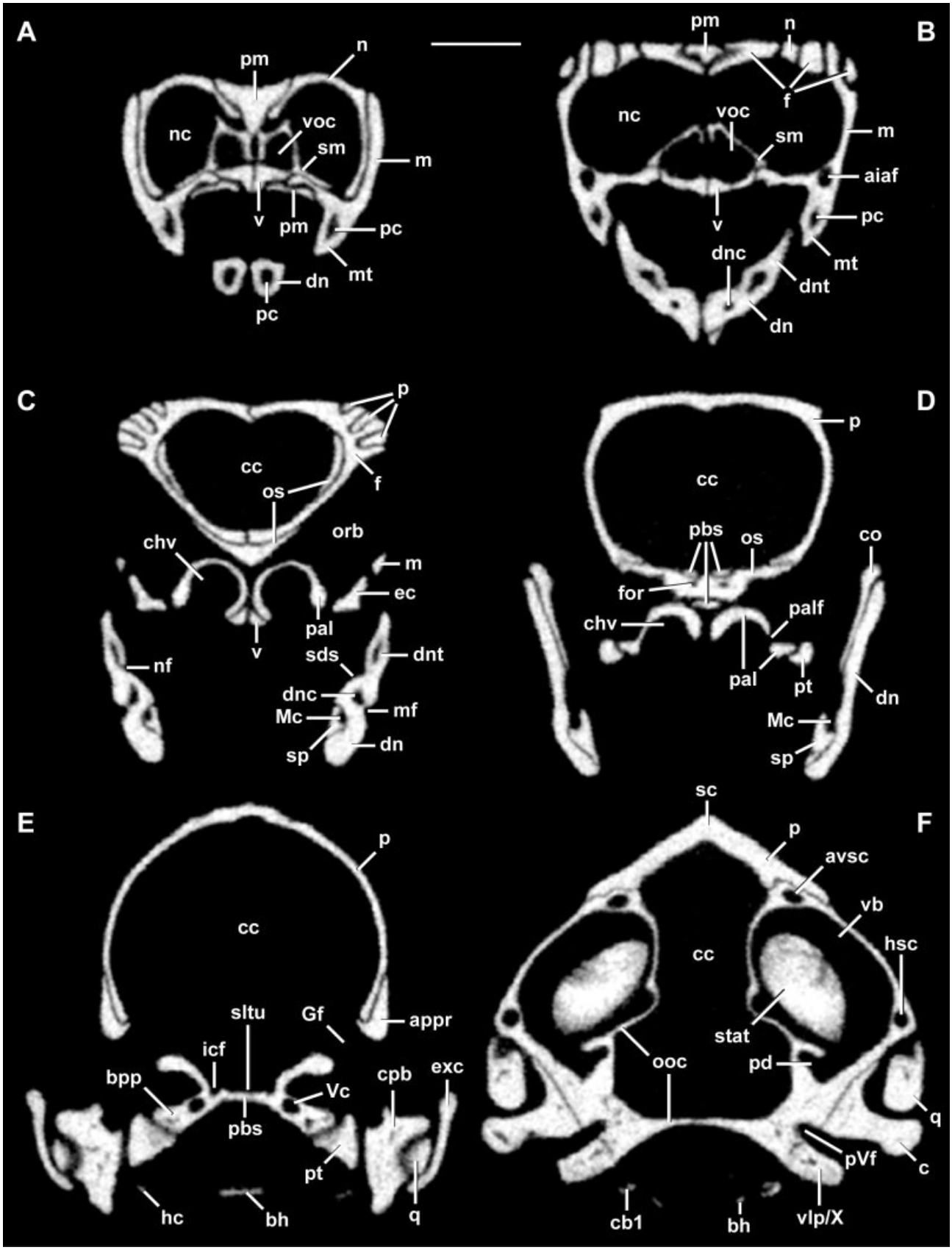
A
pm
n
nc
voc
sm
m
v
pm
pc
mt
dn
pc
B
pm
n
f
nc
voc
sm
m
aiaf
v
pc
dnc
mt
dnt
dn
C
p
cc
os
f
orb
chv
m
ec
pal
v
nf
sds
dnt
dnc
mf
Mc
dn
sp
D
p
cc
pbs
os
co
for
palf
chv
pal
pt
dn
Mc
sp
E
p
cc
sltu
Gf
appr
icf
bpp
cpb
exc
Vc
pbs
pt
hc
bh
q
F
sc
p
avsc
vb
hsc
cc
stat
ooc
pd
q
pVf
c
cb1
bh
vlp/X

Figure 2

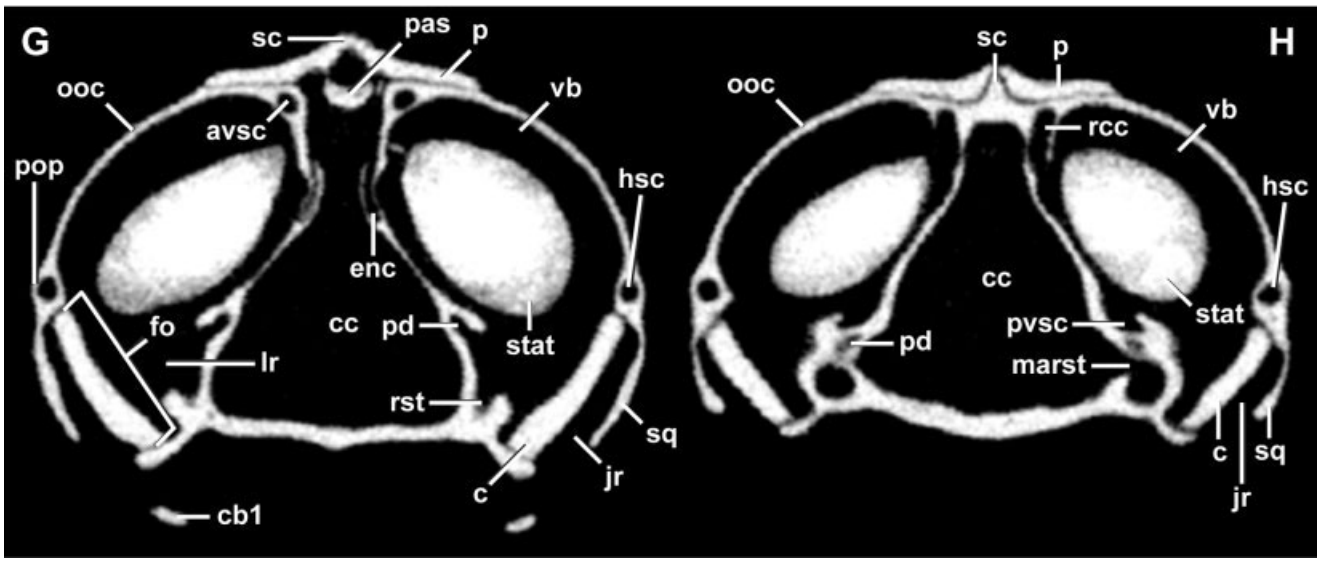

Fig. 2. *Diplometopon zarudnyi* (FMNH 64429). Selected transverse (Tra) HRXCT slices. **A:** Tra 075, **B:** Tra 105, **C:** Tra 175, **D:** Tra 212, **E:** Tra 282, **F:** Tra 333, **G:** Tra 375, **H:** Tra 391. Scale bar = 1 mm. aiaf, anterior inferior alveolar foramen; appr, alar process of prootic; avsc, anterior vertical semicircular canal; bh, basihyal; bpp, basipterygoid process; c, columella; cb1, first ceratobranchial; cc, cranial cavity; chv, choanal vault; co, coronoid; cpb, compound bone; dn, dentary; dnc, dentary canal; dnt, dentary tooth; ec, ectopterygoid; enc, endolymphatic canal; exc, extracolumella; f, frontal; fo, fenestra ovale; for, foramen; Gf, Gasserian foramen; hc, hyoid cornu; hsc, horizontal semicircular canal; icf, internal carotid foramen; jr, jugular recess; lr, lagenar recess; m, maxilla; marst, medial aperture of recessus scalae tympani; Mc, Meckelian canal; mf, mental foramen; mt, maxillary tooth; n, nasal; nc, nasal chamber; nf, nutritive foramen; ooc, otic–occipital complex; orb, orbit; os, orbitosphenoid; p, parietal; pal, palatine; palf, palatine foramen; pas, processus ascendens of supraoccipital; pbs, parabasisphenoid; pc, pulp cavity; pd, perilymphatic duct; pm, premaxilla; pop, paroccipital process; pt, pterygoid; pVf, posterior Vidian foramen; pvsc, posterior vertical semicircular canal; q, quadrate; rcc, recessus crus communis; rst, recessus scalae tympani; sc, sagittal crest; sds, subdental shelf; sltu, sella turcica; sm, septomaxilla; sp, splenial; sq, squamosal; stat, statolithic mass; v, vomer; vb, vestibule; Vc, Vidian canal; vlp, ventrolateral process; voc, vomeronasal chamber; X, "element X."

anterior to the mouth and significantly overhangs the mandible (Fig. 5A). Other amphisbaenians have a pointed or rounded snout, but in the "spade-headed" trogonophids the snout forms a broad, squared-off wedge (Fig. 5E) whose leading edge is oriented horizontally and protrudes beyond the borders of the nares.

For descriptive purposes, the skull can be divided into facial and cranial segments, with a strong craniofacial deflection angle delimiting the two (Fig. 5B). Whereas the facial segment in *Diplometopon* superficially bears a striking resemblance to *Rhineura* (Kearney et al., 2005) (and a number of other amphisbaenians [Kearney, 2003]), its underlying structure and the anatomical relations among its parts are quite different. The facial segment is composed of the premaxilla, septomaxilla, maxilla, nasal, frontal, and the anterior portion of the parietal and palate. Gans (1960) found no external evidence of the septomaxilla and questioned its presence in *Diplometopon*, but this element was identified by El-Assy and Al-Nassar (1976). The HRXCT data confirm its presence, wholly enclosed within the nasal chamber, lying lateral to the premaxillary nasal process, dorsal to the vomer and maxillary palatal process, and ventral to the nasal. There is no prefrontal, jugal, or lacrimal.

The median premaxilla is dorsoventrally flattened to form the sharp leading edge or rostral blade of the "spade snout" and covers the full width of the leading edge of the snout (Fig. 5C). This blade is buttressed laterally on each side by the nasals and maxillae, and medially by several palatal elements that make up a median strut of complex structure. This median strut includes contributions from the premaxilla, septomaxilla, maxilla, vomer, and palatine. Together, these bones may be in a position to transmit rostral loads to the braincase via the basipterygoid processes.

The dorsal and lateral surfaces of the facial segment intersect to form a distinct angle known as the canthus rostralis, which includes contributions from the nasal, maxilla, frontal, and parietal. This edge inclines medially as it continues posterodorsally to meet its counterpart at the parietal apical process (Fig. 5C). In life, the entire surface of the face between the canthi rostrali is covered by thickened, heavily keratinized scales (Kearney, 2003). These form a sharp edge at the canthus rostralis, which is used to scrape soil from the sides of the tunnel wall during burrowing.

Together, the premaxilla, maxilla, and nasal form the border around the external naris. As in other

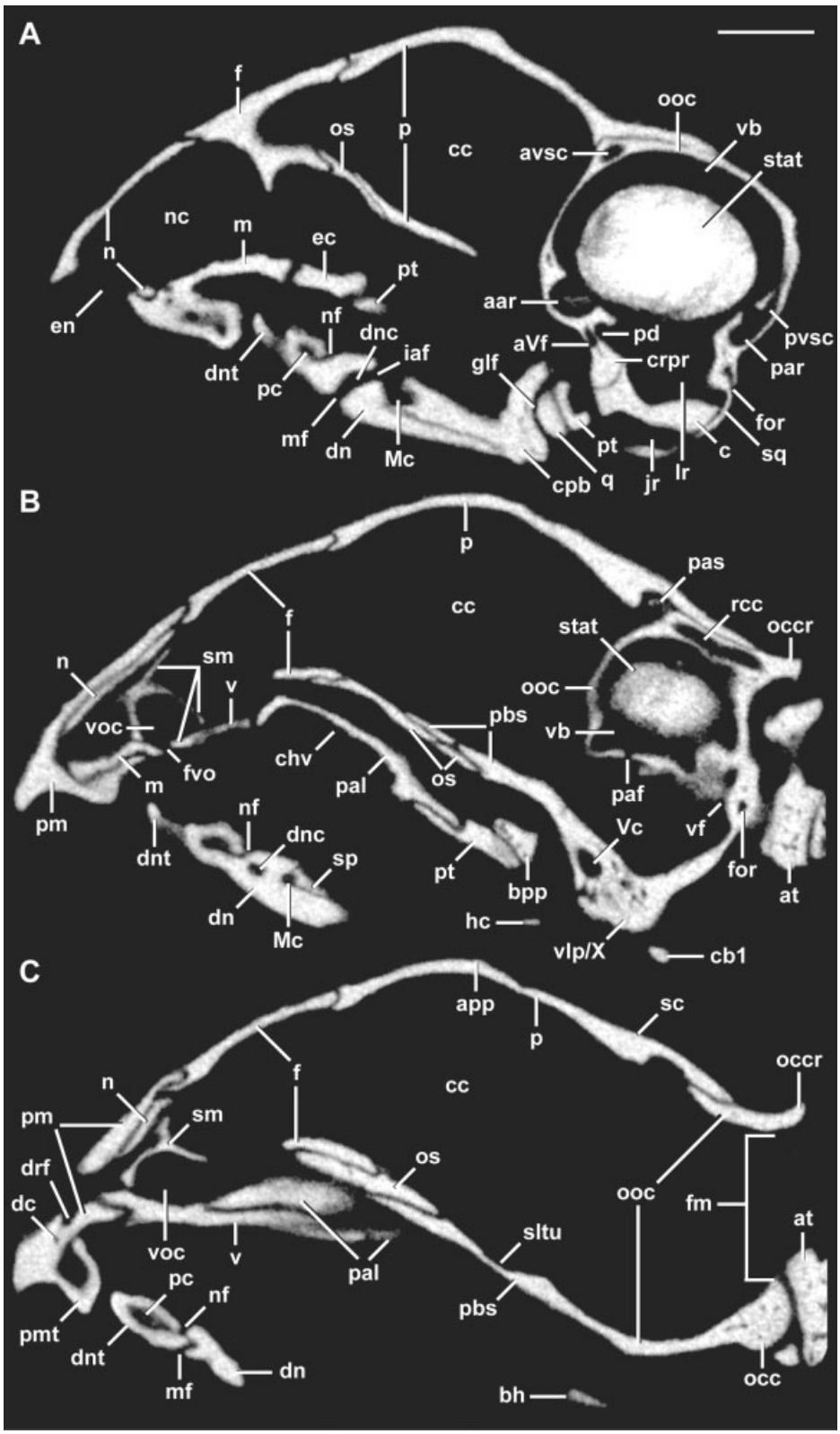

Fig. 3. *Diplometopon zarudnyi* (FMNH 64429). Selected sagittal (Sag) HRXCT slices. **A:** Sag 062, **B:** Sag 090, **C:** Sag 121. Scale bar = 1 mm. aar, anterior ampullary recess; app, apical process; at, atlas; aVf, anterior Vidian foramen; avsc, anterior vertical semicircular canal; bh, basihyal; bpp, basipterygoid process; c, columella; cb1, first ceratobranchial; cc, cranial cavity; chv, choanal vault; cpb, compound bone; crpr, crista prootica; dc, dental canal; dn, dentary; dnc, dentary canal; dnt, dentary tooth; drf, dorsal rostral foramen; ec, ectopterygoid; en, external naris; f, frontal; fm, foramen magnum; for, foramen; fvo, fenestra vomeronasalis; glf, glenoid fossa; hc, hyoid cornu; iaf, inferior alveolar foramen; jr, jugular recess; lr, lagenar recess; m, maxilla; Mc, Meckelian canal; mf, mental foramen; n, nasal; nc, nasal chamber; nf, nutritive foramen; occ, occipital condyle; occr, occipital crest; ooc, otic–occipital complex; os, orbitosphenoid; p, parietal; paf, posterior auditory foramen; pal, palatine; par, posterior ampullary recess; pas, processus ascendens of supraoccipital; pbs, parabasisphenoid; pc, pulp cavity; pd, perilymphatic duct; pm, premaxilla; pmt, premaxillary tooth; pt, pterygoid; pvsc, posterior vertical semicircular canal; q, quadrate; rcc, recessus crus communis; sc, sagittal crest; sltu, sella turcica; sm, septomaxilla; sp, splenial; sq, squamosal; stat, statolithic mass; v, vomer; vb, vestibule; Vc, Vidian canal; vf, vagus foramen; vlp, ventrolateral process; voc, vomeronasal chamber; X, "element X."

"spade-headed" amphisbaenians (Kearney, 2003), the naris in *Diplometopon* opens ventrolaterally (Fig. 5B), in contrast to the anterolateral opening found in many "round-headed" amphisbaenians (Montero and Gans, 1999) or the ventral opening found in "shovel-headed" rhineurids (Kearney, 2003; Kearney et al., 2005). Behind the external naris, the lateral wall of the facial portion of the skull is

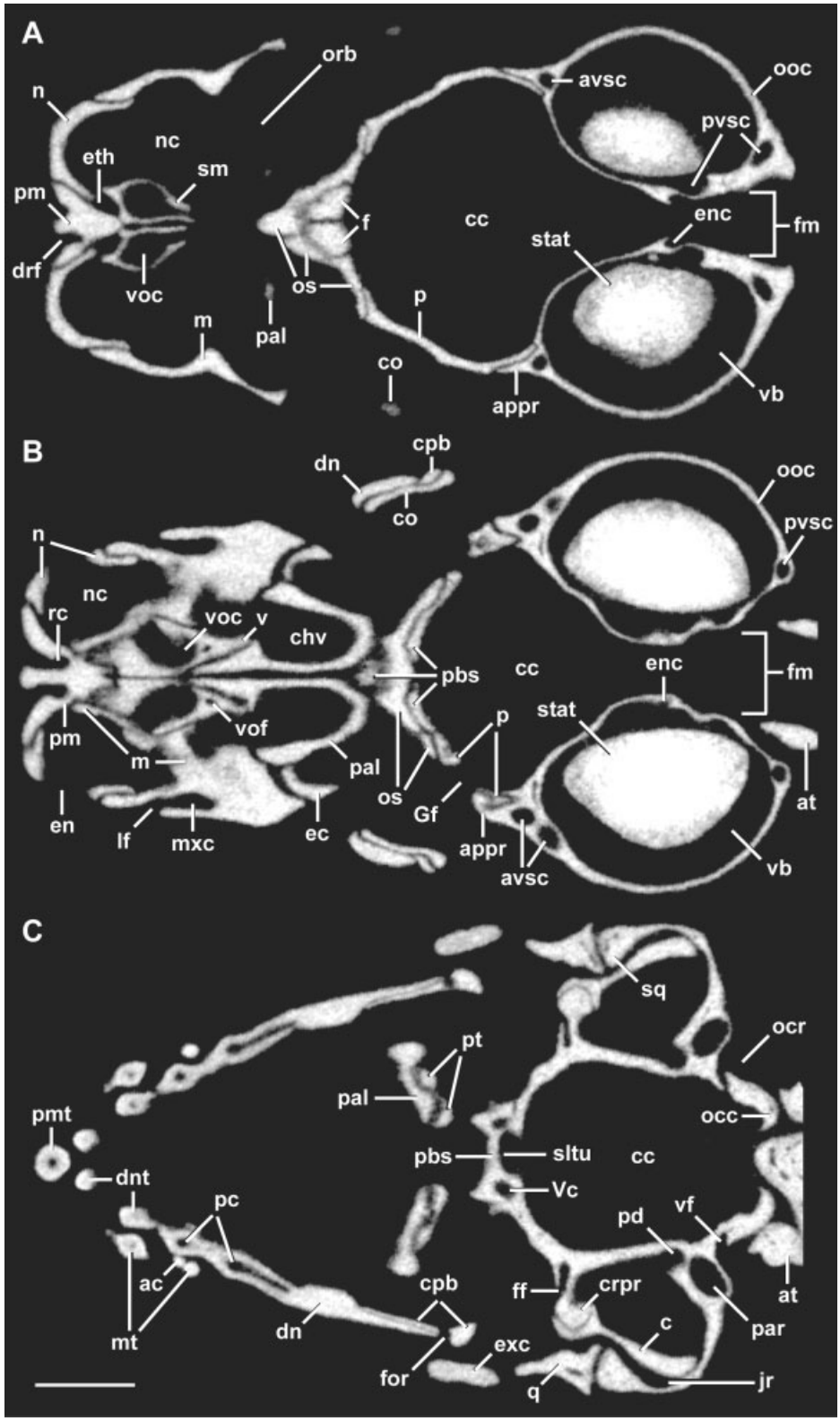

Fig. 4. *Diplometopon zarudnyi* (FMNH 64429). Selected frontal (Fro) HRXCT slices. **A:** Fro 107, **B:** Fro 132, **C:** Fro 178. Scale bar = 1 mm. ac, accessory cusp; appr, alar process of prootic; at, atlas; avsc, anterior vertical semicircular canal; c, columella; cc, cranial cavity; chv, choanal vault; co, coronoid; cpb, compound bone; crpr, crista prootica; dn, dentary; dnt, dentary tooth; drf, dorsal rostral foramen; ec, ectopterygoid; en, external naris; enc, endolymphatic canal; eth, ethmoid passageway; exc, extracolumella; f, frontal; ff, facial foramen; fm, foramen magnum; for, foramen; Gf, Gasserian foramen; jr, jugular recess; lf, labial foramen; m, maxilla; mt, maxillary tooth; mxc, maxillary canal; n, nasal; nc, nasal chamber; occ, occipital condyle; ocr, occipital recess; ooc, otic–occipital complex; orb, orbit; os, orbitosphenoid; p, parietal; pal, palatine; par, posterior ampullary recess; pbs, parabasisphenoid; pc, pulp cavity; pd, perilymphatic duct; pm, premaxilla; pmt, premaxillary tooth; pt, pterygoid; pvsc, posterior vertical semicircular canal; q, quadrate; rc, rostral canal; sltu, sella turcica; sm, septomaxilla; sq, squamosal; stat, statolithic mass; v, vomer; vb, vestibule; Vc, Vidian canal; vf, vagus foramen; voc, vomeronasal chamber; vof, vomerine foramen.

formed by the maxilla along with a small contribution from the nasal. However, in contrast to most squamates, the maxilla contributes little directly to the lateral wall of the nasal chamber. Instead, the nasal forms both the dorsal and lateral walls of the nasal chamber, while the septomaxilla lines its medial and ventral walls anteriorly, and the maxilla forms its floor posteriorly.

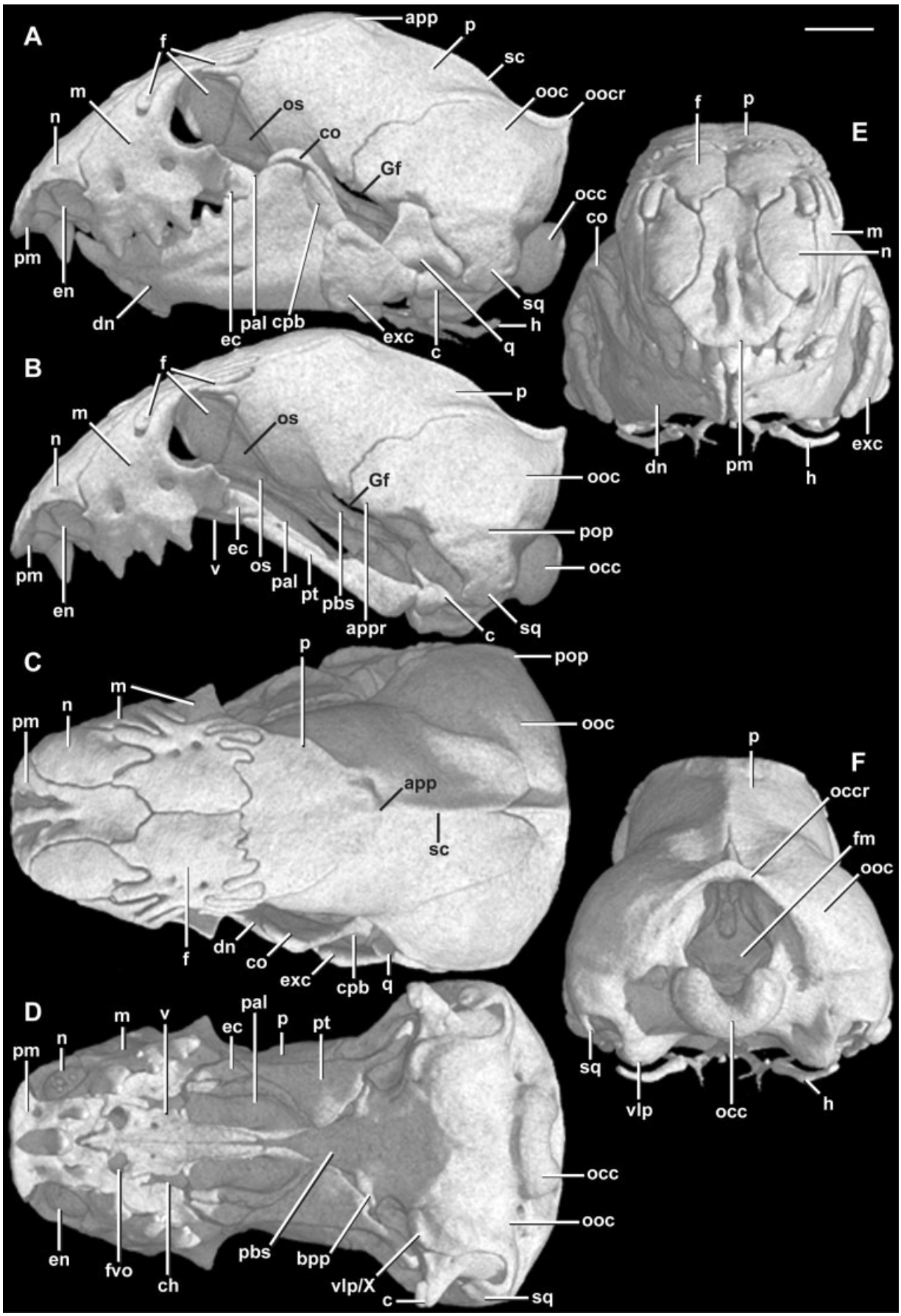
A
app
p
sc
f
m
n
os
co
ooc
oocr
Gf
occ
pm
en
dn
ec
pal
cpb
exc
c
q
sq
h
B
f
p
m
n
os
ooc
Gf
pop
ec
v
os
occ
pal
pt
pbs
pm
en
appr
c
sq
C
p
pop
m
n
pm
ooc
app
sc
f
dn
co
exc
cpb
q
D
pal
m
v
ec
p
pt
pm
n
occ
ooc
en
fvo
ch
pbs
bpp
vlp/X
c
sq
E
f
p
m
n
co
occ
exc
dn
pm
h
F
p
occr
fm
ooc
sq
vlp
occ
h

Figure 5

The nasals are completely separated from each other by the premaxillary nasal process, which extends posteriorly to contact the frontals (Gans, 1960; Kearney, 2003). The premaxilla is inscribed by deep bilateral grooves connecting foramina that communicate with the nasal cavity. The nasal extends posteriorly over the frontal as a sharp lappet that tapers to a point at the level of the posterodorsal limit of the premaxillary nasal process (Fig. 5C). The nasal fits into a V-shaped depression in the anterior margin of the adjacent frontal.

The eye in *Diplometopon* is reduced but still functional (Gans, 1960). The orbit faces laterally and is roofed by the supraorbital ridge of the frontal dorsal plate (Fig. 5B). The orbital wall is formed anteriorly by the maxillary orbital process, while the maxilla, ectopterygoid, and palatine contribute to the orbital floor, and the frontal descending process forms the medial orbital wall. The orbital rim is incomplete posteriorly.

The palate is surrounded on three sides by the upper dentition, there being no palatal teeth (Fig. 5D). There are three teeth in the premaxilla and three acrodont teeth in each maxilla, which are met by six acrodont teeth in each dentary. The palate is formed by the premaxilla, maxilla, pterygoid, ectopterygoid, palatine, and vomer. There is no palatal vacuity, and the pyriform recess is narrow and roofed by a long parabasisphenoid cultriform process. The fenestra vomeronasalis is bounded by a slight contribution from the premaxilla anteriorly, the maxilla laterally, and the vomer on all other sides. This passageway communicates with a voluminous vomeronasal (Jacobson's) chamber. Posterior to the fenestra vomeronasalis the choana is bounded by the vomerine horizontal wing medially, the maxillary palatal shelf laterally, and the palatine posteriorly (Fig. 5D). The choana is separated from the fenestra vomeronasalis by contact between the vomerine horizontal wing and the maxillary palatal shelf. The premaxilla, septomaxilla, nasal, and vomer all contribute to a complex internasal septum, which divides the nasal chamber into right and left passageways from the external naris posteriorly to the level of the first maxillary tooth.

In *Diplometopon*, as in other amphisbaenians (Zangerl, 1944; Montero and Gans, 1999), the cranial segment of the mature skull mainly comprises the parietal and a single continuous element known as the otic–occipital complex (Fig. 5B). The latter is composed of bones that develop from distinct ossification centers and that generally remain separate throughout at least a portion of postnatal ontogeny in other squamates. These include the median supraoccipital and basioccipital and the paired exoccipital and prootic (Montero et al., 1999). In *Diplometopon*, as in *Rhineura* (Kearney et al., 2005), these bones are also coossified with the basicranial axis (parabasisphenoid) and squamosal.

The roof of the cranial segment is formed anteriorly by the parietal (Fig. 5C). An anterior triangular portion of the parietal is deflected onto the facial plane of the skull. Just posterior to this, a sagittal crest runs posteriorly over the dorsal surface of the parietal, and continues along the otic–occipital complex to the back of the skull. The cranial segment is widest across the otic region, at the level of the paroccipital processes, and tapers anteriorly to its narrowest constriction at its junction with the facial segment. The otic capsule is proportionally enormous. The foramen magnum is tall and weakly triangular and roofed by the occipital crest (Fig. 5F). The occipital condyle is U-shaped and strongly developed as compared to most other squamates.

The otic–occipital complex is flanked by the temporal area, which is unenclosed in contrast to the condition in most squamates. A squamosal is not evident in external view and was not discussed by Gans (1960). However, the HRXCT data show the presence of a squamosal in *Diplometopon* (Fig. 5B), its dorsal edge fused along most of its length to the otic–occipital complex. A coossified squamosal was also identified in *Rhineura* (Kearney et al., 2005). In comparison to other squamates the squamosal in *Diplometopon* is displaced ventrally, extending to the level of the columellar shaft. The quadrate is a short, robust element (Fig. 5A). Its broad proximal cephalic condyle articulates loosely with the otic capsule and squamosal. The long axis of the quadrate is oriented anteromedially, ending in a mandibular condyle that forms a saddle-shaped articulation with the mandible. The extracolumella is greatly enlarged and fully mineralized into a triangular plate (Fig. 5A). It articulates proximally with the columellar shaft and extends distally to partially cover the lateral aspect of the quadrate and mandible (Fig. 5E).

The mandible (Fig. 5A) is a robust compound element that is formed almost entirely by the dentary, as in trogonophids generally (Gans, 1960; Kearney, 2003). The mandibular teeth occlude entirely medial to the maxillary teeth in a one-to-one correspondence; such occlusion is highly unusual in squa-

Fig. 5. *Diplometopon zarudnyi* (FMNH 64429). Three-dimensional digital reconstruction of specimen with flesh rendered transparent in (**A**) lateral, (**B**) lateral with mandible removed, (**C**) dorsal, (**D**) ventral with mandible removed, (**E**) anterior, and (**F**) posterior views. Anterior to left in A–D. Scale bar = 1 mm. app, apical process of parietal; appr, alar process of prootic; bpp, basipterygoid process; c, columella; ch, choana; co, coronoid; cpb, compound bone; dn, dentary; ec, ectopterygoid; en, external naris; exc, extracolumella; f, frontal; fm, foramen magnum; fvo, fenestra vomeronasalis; Gf, Gasserian foramen; h, hyobranchium; m, maxilla; n, nasal; occ, occipital condyle; occr, occipital crest; ooc, otic–occipital complex; os, orbitosphenoid; p, parietal; pal, palatine; pbs, parabasisphenoid; pm, premaxilla; pop, paroccipital process; pt, pterygoid; q, quadrate; sc, sagittal crest; sq, squamosal; v, vomer; vlp, ventrolateral process; X, "element X."

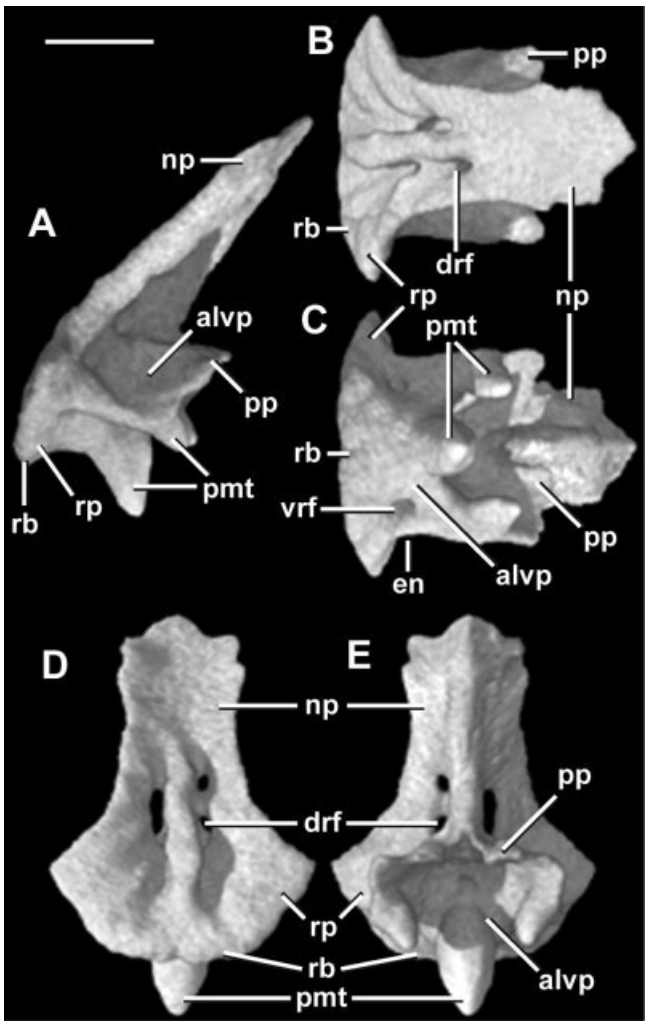

Fig. 6. Premaxilla in (**A**) lateral, (**B**) dorsal, (**C**) ventral, (**D**) anterior, and (**E**) posterior views. Anterior to left in A–C. Scale bar = 1 mm. alvp, alveolar plate; drf, dorsal rostral foramen; en, external naris; np, nasal process; pmt, premaxillary teeth; pp, palatal process; rb, rostral blade; rp, rostral process; vrf, ventral rostral foramen.

mates (Schwenk, 2000). The dentaries are unfused where they meet at the anterior midline (Fig. 5E), and the anteroventral corner of each dentary extends ventrally to a pronounced point (Fig. 5A). Behind the tooth row the mandible bears a tall coronoid process in a mechanical configuration that most likely affords a powerful bite (Gans, 1960). There is no retroarticular process; the posterior margin of the mandible *is* the glenoid fossa.

Individual Elements of the Skull

Premaxilla (Fig. 6; Tra 002–114). As in all other amphisbaenians, the premaxilla in *Diplometopon* is an azygous element with complex relations to the surrounding bones. Externally, it contacts the maxillae ventrolaterally, the vomers posteroventrally, the nasals dorsolaterally, and the frontals posterodorsally. Contact between the premaxilla and frontals distinguishes *Diplometopon* from *Rhineura* (Kearney et al., 2005) and *Amphisbaena* (Montero and Gans, 1999); this is a condition that uniquely diagnoses trogonophid amphisbaenians (Kearney, 2003). Internally, the premaxilla is contacted by the vomers dorsally and the maxillae and septomaxillae dorsolaterally. Inside the nasal chamber the premaxillary nasal process separates the septomaxillae anteriorly (Tra 065), then lies dorsal to them posteriorly (Fig. 2B).

For comparative purposes, we describe the premaxilla as being organized around its alveolar plate (=basal plate of Montero and Gans, 1999). In *Diplometopon*, as in *Rhineura* (Kearney et al., 2005), the alveolar plate supports three tooth positions. This is in contrast to the alveolar plate in *Amphisbaena*, which holds seven teeth (Montero and Gans, 1999). Viewed from below, the alveolar plate is rectangular and its teeth are arranged in a shallow V-shaped pattern (Fig. 6C). The most anterior premaxillary tooth is by far the largest, a condition characteristic of amphisbaenians generally (Gans, 1978; Estes et al., 1988; Kearney, 2003). The smaller teeth on either side are more posteriorly placed and more posteriorly inclined. The dorsolateral surfaces of the alveolar plate lie in apposition with the ventromedial surfaces of the maxillary premaxillary processes (Tra 045). This simple overlap is also present in *Amphisbaena* (Montero and Gans, 1999) but contrasts with the more elaborately intertongueing articulation between these bones in *Rhineura* (Kearney et al., 2005).

The alveolar plate projects forward, then expands into its distinctive rostral process. This structure, which forms the entire rostral blade of the "spade snout" in *Diplometopon*, is absent in most amphisbaenians (e.g., *Amphisbaena*; Montero and Gans, 1999), but a closely comparable structure is developed in a few others (e.g., *Rhineura*; Kearney et al., 2005). Current phylogenetic hypotheses (Kearney, 2003; Kearney and Stuart, 2004) suggest that this distinctive rostral blade evolved convergently in rhineurid and trogonophid amphisbaenians.

The nasal process rises dorsally from the rostral process (Fig. 6D). The nasal process is approximately the same width throughout its length, as it runs posteriorly between the nasals to the point where it contacts the frontals at their midline (Tra 084). The nasal process is completely exposed on the surface of the skull in *Diplometopon*, whereas the nasals obscure it from view partially in *Amphisbaena* (Montero and Gans, 1999) and completely in *Rhineura* (Kearney et al., 2005). The anterodorsal surface of the premaxilla is inscribed by a pair of grooves that begin shallowly on the rostral process, deepen as they extend posteriorly along the nasal process, then shallow again before they terminate at approximately the midpoint of the nasal process.

Each groove houses a dorsal rostral foramen, which is subdivided on the left side of this specimen. The posterior end of the nasal process fits into a depression on the anteromedial corner of each frontal (Fig. 2B), where it abruptly tapers to a point.

In most squamates the alveolar and nasal processes make substantial contributions to the narial border, while the superior surface of the alveolar plate forms the floor of the naris (Oelrich, 1956); this condition persists in *Amphisbaena* (Montero and Gans, 1999). However, in many "spade-headed" amphisbaenians, including *Diplometopon*, the external naris is displaced such that it opens from the ventrolateral surface of the rostrum and has no floor (Fig. 5B). The premaxillary rostral process contributes to the narial border, but most of the border circumference is built by the maxillary rostral spine and the nasal (Fig. 4B). When viewed from below, the premaxilla can be seen to widely separate the external nares on the ventral face of the rostrum (Fig. 6C), but the intervention by the maxillary rostral spine almost completely separates the premaxilla from the narial border.

The premaxilla continues onto the palate as a pair of moderately developed, divergent palatal processes (=lateral process of Montero and Gans, 1999) that extend to the level of the first maxillary tooth (Tra 082). The palatal process lies ventrolateral to the vomer and lines the inferior surface of the maxillary palatal shelf (Fig. 2A). The premaxillary palatal process is absent or weakly developed in many amphisbaenians, but is extremely well developed in rhineurids (Berman, 1976; Kearney, 2003; Kearney et al., 2005).

The premaxilla is penetrated by a rostral canal (=longitudinal canal of Montero and Gans, 1999) that opens from the medial wall of the nasal chamber via the septomaxillary apical foramen (Tra 062). The canal passes anteriorly for a short distance before penetrating the premaxilla at the juncture of the nasal process and alveolar plate (Tra 039). These canals then emerge as paired dorsal rostral foramina on the anterodorsal surface of the premaxilla just dorsal to the alveolar plate (Fig. 4B), and as paired ventral rostral foramina on the ventral surface of the alveolar plate at its junction with the rostral process (Fig. 6C). The ventral rostral foramina are also present in *Rhineura* (Kearney et al., 2005) but not in *Amphisbaena* (Montero and Gans, 1999). The rostral canal likely transmits cutaneous branches of the medial ethmoidal nerve, an anterior extension of the maxillary nerve (V2), and a rostral branch of the maxillary artery (Oelrich, 1956). Three dental canals penetrate ventrally into the premaxilla from the floor of the rostral canals (Tra 036), each supplying a premaxillary tooth locus (Fig. 3C).

Septomaxilla (Fig. 7; Tra 057–116). The septomaxilla is a paired element in *Diplometopon* that lies entirely within the nasal chamber, where it contacts the premaxilla, maxilla, vomer, and nasal. The

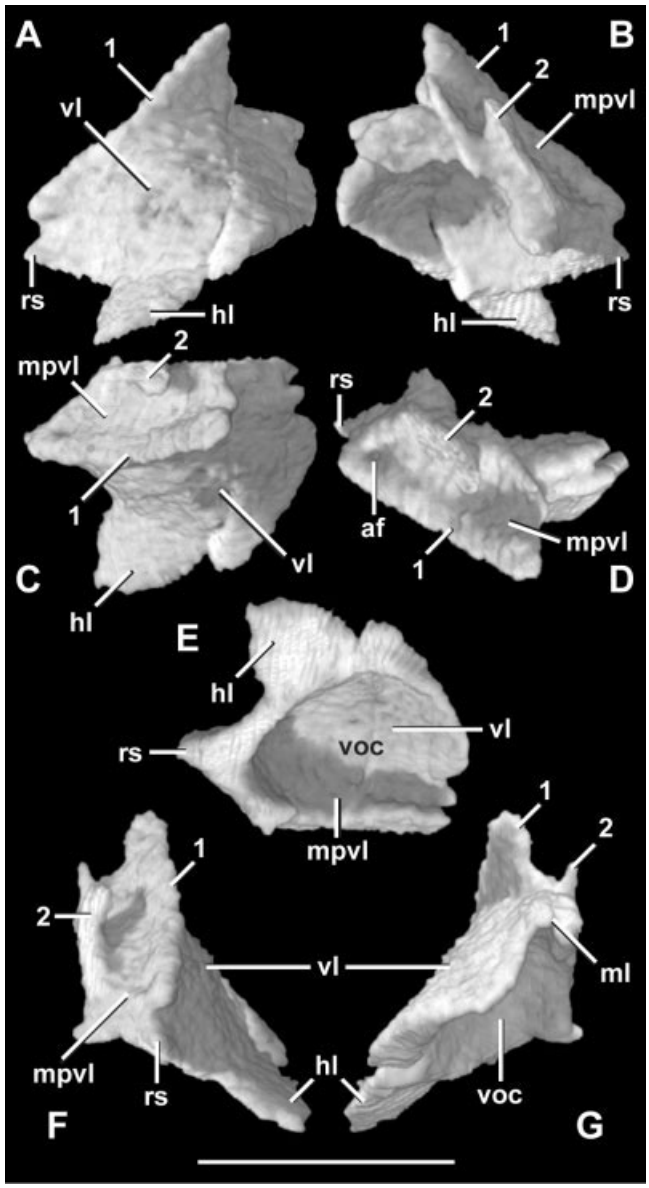

Fig. 7. Left septomaxilla in (**A**) lateral, (**B**) medial, (**C**) dorsal, (**D**) oblique dorsal, (**E**) ventral, (**F**) anterior, and (**G**) posterior views. Scale bar = 1 mm. af, apical foramen; hl, horizontal lamina; mpvl, median process of vertical lamina; rs, rostral spine; vl, vertical lamina; voc, vomeronasal chamber; 1, ridge at juncture of median process and vertical lamina; 2, ridge along dorsal edge of median process.

septomaxilla is of complex shape, comprising a vertical lamina that contributes to the internasal septum and roofs the vomeronasal chamber, and a horizontal lamina that spreads to form a partial floor to the nasal chamber (Figs. 2A, 7A). A median process projects anteriorly from the dorsal edge of the vertical lamina, turning ventrally to abut its counterpart at the midline (where they are separated by a cartilaginous nasal septum), forming a highly vaulted vomeronasal chamber (Figs. 2A, 7E). The juncture of the median process with the vertical

lamina is marked by a pronounced anteroposterior ridge (Fig. 7C). A smaller ridge runs along the median process for most of its length (Fig. 7E), contacting the premaxillary nasal process (Fig. 2A). The median process of the vertical lamina gradually diminishes in size posteriorly.

The vertical lamina narrows anteriorly to a short rostral spine (Fig. 7A) that extends to roughly the midpoint of the naris (Fig. 4A) and contributes to the medial wall of the internarial girder. The septomaxillary rostral spine is also present in *Rhineura* (Kearney et al., 2005) but not in *Amphisbaena* (Montero and Gans, 1999). The rostral spine also contributes to the lateral wall of the short, paired ethmoid passageway, a median longitudinal channel affording passageway from the nasal chamber to the alveoli and the surface of the face. Its opening is the apical foramen (=longitudinal passage of Montero and Gans, 1999) (Tra 062) (Fig. 7D), from which it passes for a short distance along the internarial girder before penetrating the premaxilla as the rostral canal (Tra 039). The septomaxilla forms the lateral wall of the ethmoid passageway while the nasal and premaxilla form its roof, the premaxilla forms its medial wall, and the vomer forms its floor. The ethmoid passageway conveys premaxillary and ethmoid branches of the trigeminal nerve to the premaxillary dentition and cutaneous tissues of the rostrum, respectively.

The vertical lamina bends sharply at its base (Fig. 7E), where it spreads laterally onto the floor of the nasal passage as the horizontal lamina (=lateral process of Montero and Gans, 1999) (Fig. 2A). The horizontal lamina lies dorsal to the maxillary palatal process, tapering posteriorly and terminating at the level of the vomerine horizontal wing.

The septomaxilla in *Diplometopon* is much more complex than that in *Amphisbaena* (Montero and Gans, 1999). It is similar to the septomaxilla in *Rhineura* (Kearney et al., 2005) in being divided into distinct vertical and horizontal laminae and in its general relations to the nasal septum and vomeronasal chamber. However, the septomaxilla in *Diplometopon* is comparatively foreshortened. As a result, the apical foramen and ethmoid passageway lie largely dorsal to the vomeronasal chamber, whereas in *Rhineura* both structures lie anterior to the vomeronasal chamber.

Maxilla (Fig. 8; Tra 035–178). As in amphisbaenians generally, the paired maxilla in *Diplometopon* is roughly triangular in lateral view (Fig. 8A) and roughly L-shaped in cross-section (Fig. 8E). It makes contact with the premaxilla, septomaxilla, vomer, palatine, ectopterygoid, nasal, and frontal. The facial process forms most of the lateral surface of the facial segment of the skull (Fig. 8A), while the palatal process contributes primarily to the anterolateral palatal roof (Fig. 8C). The two processes meet at an approximately right angle along the alveolar margin, which supports three teeth. A short, broad

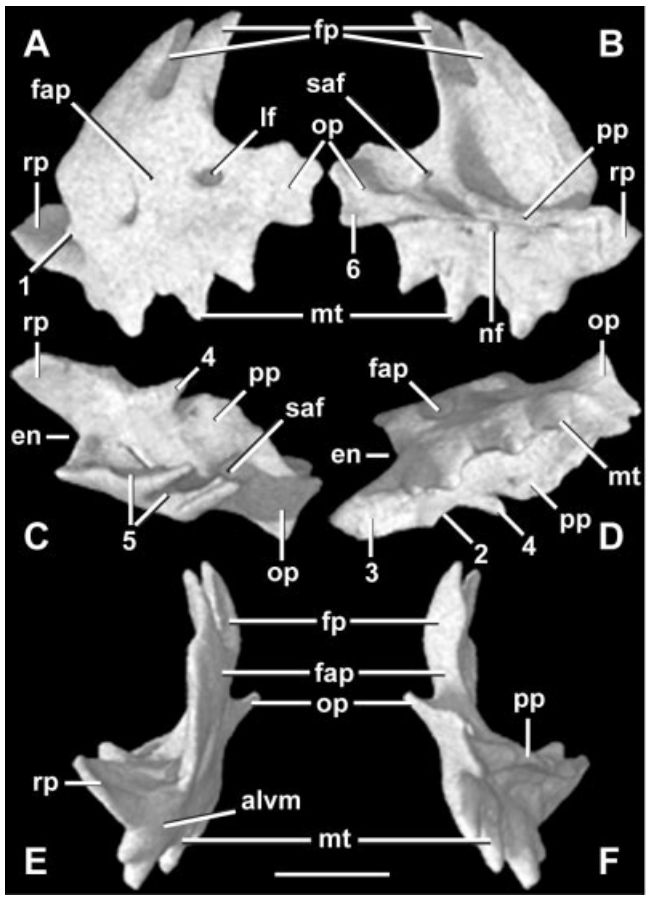

Fig. 8. Left maxilla in (**A**) lateral, (**B**) medial, (**C**) dorsal, (**D**) ventral, (**E**) anterior, and (**F**) posterior views. Scale bar = 1 mm. alvm, alveolar margin; en, external naris; fap, facial process; fp, frontal process; lf, labial foramen; mt, maxillary tooth; nf, nutritive foramen; op, orbital process; pp, palatal process; rp, rostral process; saf, superior alveolar foramen; 1, spine ventral to nasal-maxillary suture; 2, margin of choana; 3, area of overlap with premaxillary palatal process; 4, finger that contacts vomer horizontal wing; 5, notches that receive anteriorly projecting fingers of frontal; 6, area of maxilla-ectopterygoid contact.

rostral process projects anteromedially from the alveolar margin (Fig. 8C), and a short orbital process projects posteriorly from the other end of the palatal process beneath the orbit, where it contributes to the orbital floor.

The facial process (=lateral plate of Montero and Gans, 1999) expands over the side of the snout to contact the nasal anteriorly (Fig. 2A) and the frontal dorsally (Fig. 2B). It is taller than wide in *Diplometopon*, whereas the reverse is true in *Amphisbaena* (Montero and Gans, 1999) and *Rhineura* (Kearney et al., 2005). A small rostral spine projects anteriorly from the alveolar margin (Fig. 8C) where it buttresses the ventrolateral edge of the nasal (Fig. 3A). This spine most likely corresponds to the more intricate maxillary nasal process of *Rhineura* (Kearney et al., 2005). An elongate, bifurcate frontal process (Kritzinger, 1946) juts from the superior edge of

the maxillary facial process and extends posterodorsally almost to the frontoparietal suture (Tra 141). The anterior prong wedges between two fingers of the frontal (Fig. 2B), while the posterior prong lies lateral to the frontal, where it forms the anterodorsal margin of the orbit (e.g., Tra 129). A bifurcate frontal process is characteristic of trogonophids (Gans, 1960). In both *Rhineura* (Kearney et al., 2005) and *Amphisbaena* (Montero and Gans, 1999), the frontal process is unforked and abutted posteriorly by the prefrontal, which is absent in *Diplometopon*.

The maxillary canal runs longitudinally through the maxilla just above the tooth row (Tra 086–140) (Fig. 4B). It conveys the superior alveolar nerve (Oelrich, 1956), a sensory branch of the trigeminal maxillary nerve that passes from the orbit into the maxillary canal through the superior alveolar foramen (Tra 134) (Fig. 8C). As it courses through the maxilla, the maxillary canal gives off three groups of subsidiary canals, which supply innervation to the teeth, surface of the snout, and inner surface of the nasal passage. Three narrow dental canals penetrate the maxilla ventrally (e.g., Tra 121) where they supply a small nerve fiber to each maxillary tooth position. Two large labial foramina pass laterally onto the face above the teeth (Figs. 4B, 8A), conveying cutaneous branches of the superior alveolar nerve and the maxillary artery (Oelrich, 1956) to the superficial tissues of the face. Larger numbers of labial foramina occur in *Amphisbaena* (Montero and Gans, 1999) and especially in *Rhineura* (Kearney et al., 2005). The third group of subsidiary passages penetrates the maxilla ventromedially above the teeth (Fig. 8A) as a series of nutritive foramina that communicate to the tissues lining the roof of the mouth. Lastly, at its anterior terminus, the maxillary canal exits into the nasal chamber through the anterior inferior alveolar foramen (Fig. 2B). Branches of the maxillary artery and superior alveolar nerve pass through this foramen, supplying cutaneous tissues of the snout (Oelrich, 1956) and transmitting the alveolar nerve toward the septomaxillary apical foramen and premaxillary rostral canal.

The palatal process (Fig. 8C) extends medially as a horizontal shelf forming a floor beneath the nasal passage (Fig. 2A). It is overlapped medially by the septomaxilla and contacts the premaxillary palatal process anteroventrally. It approaches but does not contact the palatine posterodorsally. The medial edge of the palatal process contacts the vomerine rostral process. Behind this contact, it forms the lateral border of the fenestra vomeronasalis (Fig. 3B). Further posteriorly, along the anterior half of the vomerine horizontal wing, the palatal process forms the anterior and lateral margins of the choana (Fig. 8D). Its anterior contribution to this margin is formed by a posteromedially projecting finger of the maxillary palatal process (Tra 111) that contacts the vomerine horizontal wing. This finger also contacts the ventral edge of the septomaxillary vertical lamina. The rostral process (=premaxillary process of Montero and Gans, 1999) (Fig. 8D) extends anteromedially to lie along the dorsolateral surface of the premaxillary alveolar plate. Its dorsomedial edge contacts the vomerine rostral process (e.g., Tra 059).

The junction of the facial and palatal processes marks the maxillary alveolar margin. Three acrodont teeth occupy this margin, the first (and largest) near the anterior margin of the facial process and the last just anterior to the orbit (Fig. 8A). This reduced number of maxillary teeth contrasts with the six in *Rhineura* (Kearney et al., 2005) and the five in *Amphisbaena* (Montero and Gans, 1999). The teeth are fused at their bases by extensive bone of attachment, and several give the impression of having small accessory cusps (Fig. 4C). The crowns are slightly inclined posteriorly (Fig. 8A).

The short orbital process lies in simple articulation with the anterolateral surface of the ectopterygoid (Figs. 2C, 8B), extending posteriorly to the level of the frontoparietal suture. It is much shorter than the orbital process in *Rhineura* (Kearney et al., 2005), which is clasped by a bifurcate ectopterygoid maxillary process. *Amphisbaena* lacks a maxillary orbital process (Montero and Gans, 1999). Because *Diplometopon* lacks a prefrontal, the anterior and ventral margins of the orbit are formed entirely by the maxilla (Fig. 4A,B), distinguishing it from the condition in *Rhineura* (Kearney et al., 2005) and *Amphisbaena* (Montero and Gans, 1999).

Nasal (Fig. 9; Tra 018–113). The nasal is a paired, trough-shaped element that contacts the premaxilla, maxilla, and frontal; it approaches but does not contact the septomaxilla. The nasal forms the dorsal border of the external naris and the roof over the nasal chamber (Fig. 9D). It bears four processes: an anterior rostral process, a lateral facial process, a medial premaxillary process, and a posterior frontal process.

The short, broad rostral process forms the anterodorsal corner of the external naris (Figs. 4A, 9A). The facial process (=facial lamina of *Rhineura*, Kearney et al., 2005) extends posteroventrally to form the lateral wall of the nasal chamber (Fig. 2A). It lines the medial surface of the maxillary facial process; the extent of overlap by the maxilla is delimited by a ridge on the nasal (Fig. 9A). Its blunt ventral tip abuts the rostral spine on the maxillary facial process (Figs. 3A, 9E). The facial process exhibits the same topological relationships in *Rhineura*, except that its ventral tip is received by a more elaborate maxillary nasal process, and it is penetrated by three small foramina that communicate between the nasal chamber and the external surface of the snout (Kearney et al., 2005). *Amphisbaena* lacks a facial process; the lateral edge of the nasal simply abuts the dorsal edge of the maxilla (Montero and Gans, 1999).

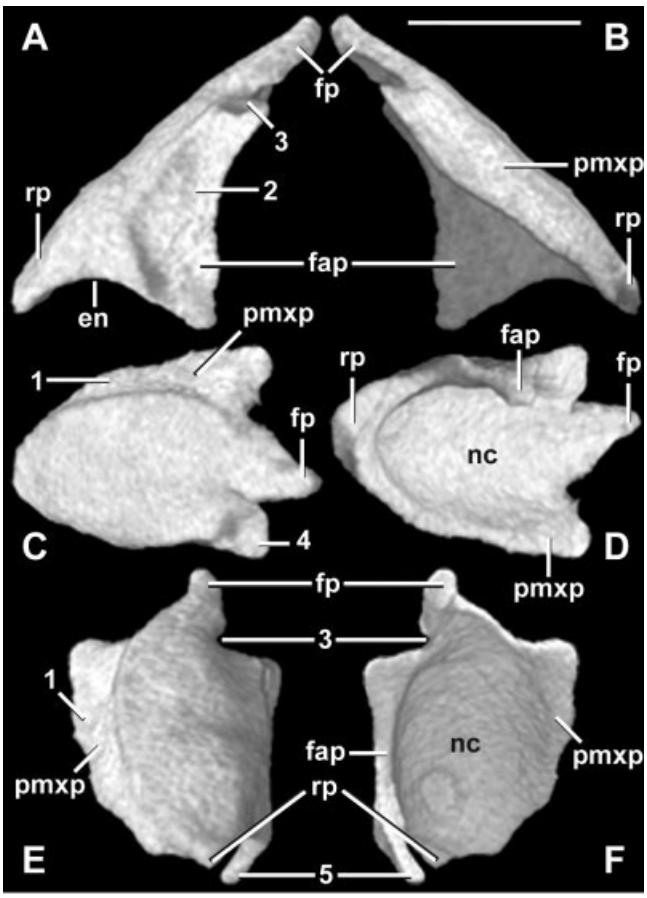

Fig. 9. Left nasal in (**A**) lateral, (**B**) medial, (**C**) dorsal, (**D**) ventral, (**E**) anterior, and (**F**) posterior views. Scale bar = 1 mm. en, external naris; fap, facial process; fp, frontal process; nc, nasal chamber; pmxp, premaxillary process; rp, rostral process; 1, shelf overlain by premaxillary nasal process; 2, shelf overlain by maxillary facial process; 3, notch closed by projecting finger of frontal to form foramen; 4, depression receiving middle forward projecting finger of frontal; 5, tip abutting spine on maxillary facial process.

Medially, a premaxillary process (=medial sheet of Montero and Gans, 1999) projects ventromedially to line the ventrolateral surface of the premaxillary nasal process (Fig. 2A); the extent of overlap by the premaxilla is delimited by a ridge on the nasal (Fig. 9C). This is similar to the condition in *Amphisbaena* (Montero and Gans, 1999), whereas in *Rhineura* the premaxillary process clasps the premaxillary nasal process, thereby obscuring it from view in the articulated skull (Kearney et al., 2005). The nasal premaxillary process in *Diplometopon* approaches but does not meet the septomaxillary vertical lamina, unlike in *Amphisbaena* (Montero and Gans, 1999) and *Rhineura* (Kearney et al., 2005).

The frontal process (Montero and Gans, 1999) projects from the posterodorsal edge of the nasal (Fig. 9C) and inserts between two anteriorly projecting fingers of the frontal (Fig. 2B), as in *Rhineura* (Kearney et al., 2005) and *Amphisbaena* (Montero and Gans, 1999). The posterodorsal corner of the nasal bears a depression that receives the tip of the middle forward projecting finger of the frontal (Fig. 9C). The frontal process extends posteriorly to the level of the distal tip of the premaxillary nasal process, terminating bluntly without overlapping the frontal. At its base, its lateral edge is notched (Fig. 9E); the middle forward-projecting finger of the frontal closes this notch to form a foramen that communicates with the nasal chamber (Tra 092). This foramen also occurs in other trogonophids (Gans, 1960). A similar foramen is formed by the nasal and frontal in *Amphisbaena*; however, it communicates with a complex series of foramina that open onto the dorsal surface of the nasal (Montero and Gans, 1999), not into the nasal chamber. No foramina penetrate the nasal in *Diplometopon*. The condition in *Rhineura* is unknown owing to postmortem erosion of the nasals in the single specimen that has been studied with HRXCT (Kearney et al., 2005).

Vomer (Fig. 10; Tra 051–202). The vomer is a paired element that forms the floor of the vomeronasal chamber. Its general configuration resembles both *Rhineura* (Kearney et al., 2005) and *Amphisbaena* (Montero and Gans, 1960) in that it contrib-

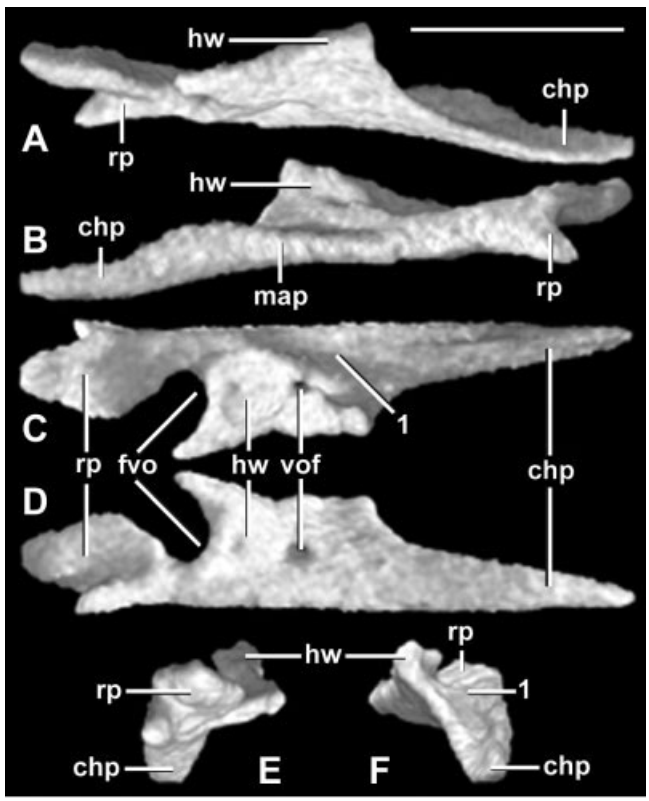

Fig. 10. Left vomer in (**A**) lateral, (**B**) medial, (**C**) dorsal, (**D**) ventral, (**E**) anterior, and (**F**) posterior views. Scale bar = 1 mm. chp, choanal process; fvo, fenestra vomeronasalis; hw, horizontal wing; map, median articular plane; rp, rostral process; vof, vomerine foramen; 1, groove that receives palatine vomerine process.

utes to the internarial girder, the roof of the palate, and the borders of the choana. The vomer is contacted medially by its counterpart, anteriorly by the premaxilla, septomaxilla, and maxilla, laterally by the maxilla, dorsally by the septomaxilla, and posterodorsally by the palatine.

A rostral process (=anterior process of Montero and Gans, 1999) (Fig. 10C) projects anteriorly, contacting the maxillary palatal process (Tra 065) and the septomaxillary vertical lamina (Tra 069). In contrast to *Rhineura* (Kearney et al., 2005) and *Amphisbaena* (Montero and Gans, 1999), its anterior extremity is deeply bifurcated where it clasps the premaxillary alveolar plate (Fig. 3C). The rostral process is triangular in cross-section and forms a robust strut extending from the midpoint of the naris to approximately the midpoint of the vomeronasal chamber (Sag 091). The rostral process abuts its counterpart posteriorly along a deep, flat, median articular plane (Figs. 2A, 10B), forming the major structural element along the ventral midline of the snout. The vomers tie together projections of the premaxilla, septomaxillae, and maxillae into a complex internarial girder that appears to brace the rostral blade, via the roof of the palate, against the basicranial axis. The rostral process abuts the maxillary palatal process, overlies the premaxillary palatal process, and underlies the septomaxillary vertical lamina (Fig. 2A), forming the anteromedial margin of the fenestra vomeronasalis (Fig. 10C). The rostral process also forms the floor of the anterior portion of the vomeronasal chamber (Fig. 2A).

The vomer expands laterally to form a broad horizontal wing (=lateral wing of Montero and Gans, 1999), which lies posterior to the rostral process at the approximate midpoint of the vomer (Fig. 10C). The horizontal wing contributes simultaneously to the roof of the palate, the floor of the vomeronasal chamber, and the posterior border of the fenestra vomeronasalis. Its lateral extremity contacts the maxillary palatal process and the septomaxillary vertical lamina (Fig. 2B). The horizontal wing projects anteriorly such that its anterior edge is deeply incised by the fenestra vomeronasalis (Fig. 4B). A similar but less extreme condition in seen in *Amphisbaena* (Montero and Gans, 1999), whereas in *Rhineura* (Kearney et al., 2005) the anterior edge of the horizontal wing slopes posterolaterally to form a more slit-like fenestra vomeronasalis. A ridge diverges laterally along the dorsal surface of the horizontal wing, marking the edge of a groove that receives the vomerine process of the palatine (Fig. 10C). A foramen pierces each vomer at the midpoint of the horizontal wing (Figs. 4B, 10D), exiting dorsally just lateral to the groove receiving the palatine vomerine process. This foramen, which is also present in *Rhineura* (Kearney et al., 2005) and *Amphisbaena* (Montero and Gans, 1999), transmits branches of the anterior palatine nerve and inferior nasal artery (Oelrich, 1956).

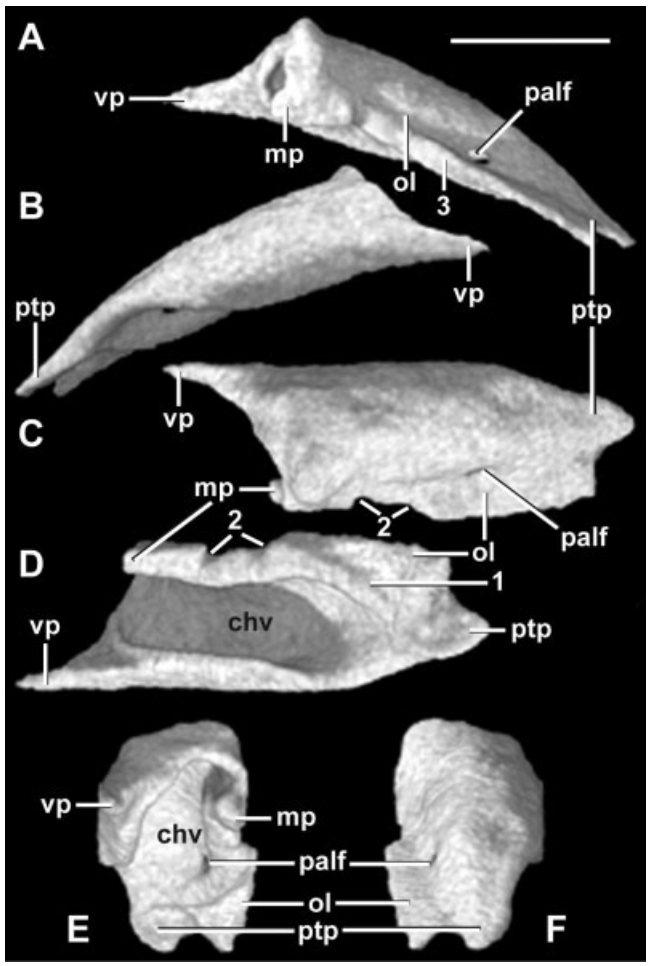

Fig. 11. Left palatine in (**A**) lateral, (**B**) medial, (**C**) dorsal, (**D**) ventral, (**E**) anterior, and (**F**) posterior views. Scale bar = 1 mm. chv, choanal vault; mp, maxillary process; ol, orbital lamina; palf, palatine foramen; ptp, pterygoid process; vp, vomerine process; 1, ridge delimiting area of overlap by pterygoid; 2, notches forming foramina in articulation with ectopterygoid; 3, area of articulation with ectopterygoid.

The right and left vomers remain in contact along the midline via a flat median articular plane (Fig. 2B) for approximately three-quarters of their length (Tra 073–169), until a very narrow pyriform recess intervenes between them. The vomer gradually tapers posteriorly into a slender choanal process (=posterior process of Montero and Gans, 1999) (Fig. 10C) that courses along the midline of the palatal roof, terminating in a thin point wedging shallowly between its counterpart and the ventromedial edge of the palatine (Fig. 2C).

Palatine (Fig. 11; Tra 111–266). The palatine is a paired element forming the roof of the choanal vault and portions of the floor of the orbit. It is inclined anteriorly to parallel the angulation of the skull (Fig. 11A). It contacts the vomer anteroventrally, the maxilla anterolaterally, the ectopterygoid laterally, and the pterygoid posteroventrally. The right and left palatines closely approach each other

anteriorly and are separated posteriorly by a very narrow pyriform recess (Fig. 4B). The palatine bears a vomerine process anteromedially, a maxillary process anterolaterally, and a pterygoid process posteriorly. In its general relations the palatine resembles that of *Rhineura* (Kearney et al., 2005) and *Amphisbaena* (Montero and Gans, 1999); however, the precise geometries of its processes differ among these taxa.

The vomerine process (=parasagittal plate of Montero and Gans, 1999) (Fig. 11A) is formed by a slender finger that projects anteromedially into a groove on the dorsal surface of the vomer, medial to the vomerine horizontal wing (Tra 119). The maxillary process (=lateral process of Montero and Gans, 1999) projects only a short distance forward (Fig. 11C), where it contacts the maxillary palatal process and the ectopterygoid (Fig. 4B). In contrast to *Rhineura* (Kearney et al., 2005) and *Amphisbaena* (Montero and Gans, 1999), the maxillary process is weakly developed in *Diplometopon*. In *Amphisbaena* the maxillary process extends far laterally, whereas in *Rhineura* it extends far anteriorly. The pterygoid process (=posterior process of Montero and Gans, 1999) projects posteriorly (Fig. 11C), where it overlies the dorsal surface of the pterygoid transverse process (Figs. 2D, 3B); this area of overlap is delimited by a ridge on the palatine (Fig. 11D). A similar relationship is seen in *Amphisbaena* (Montero and Gans, 1999), whereas in *Rhineura* (Kearney et al., 2005) the pterygoid process is also weakly forked to receive the pterygoid.

Above the roof of the choanal vault, the superior surface of the palatine approaches the overlying parabasisphenoid and frontal descending process. However, unlike in *Rhineura* (Kearney et al., 2005) and *Amphisbaena* (Montero and Gans, 1999), it does not contact either (Figs. 2C, 4B). An orbital lamina projects ventrolaterally from its superior face (Fig. 11A) to contact the ectopterygoid via a flat surface that extends along most of the length of the orbital floor (Figs. 2C, 4B). The orbital lamina is incised by two shallow notches approximately halfway back along this contact (Tra 174, 191). The notches are closed by the medial surface of the ectopterygoid to form two small foramina that communicate between the palate and the orbit (Fig. 5D). A single opening was described previously in this area in *Diplometopon* (Gans, 1960; El-Assy and Al-Nassar, 1976) and in *Amphisbaena* (Montero and Gans, 1999); the latter authors questioned whether it might represent a reduced suborbital fenestra.

The inferior surface of the palatine (Fig. 11D) is smooth and highly arched along much of its length, forming the bony roof of the choanal vault (Fig. 2C) and constituting the posterodorsal border of the choana (Jollie, 1960). The vault is tallest anteriorly, becoming shallower posteriorly until the palatine eventually flattens out, ending in its contact with the pterygoid (Fig. 11A). In life, the choanal vault is closed ventrally by connective tissue (Oelrich, 1956).

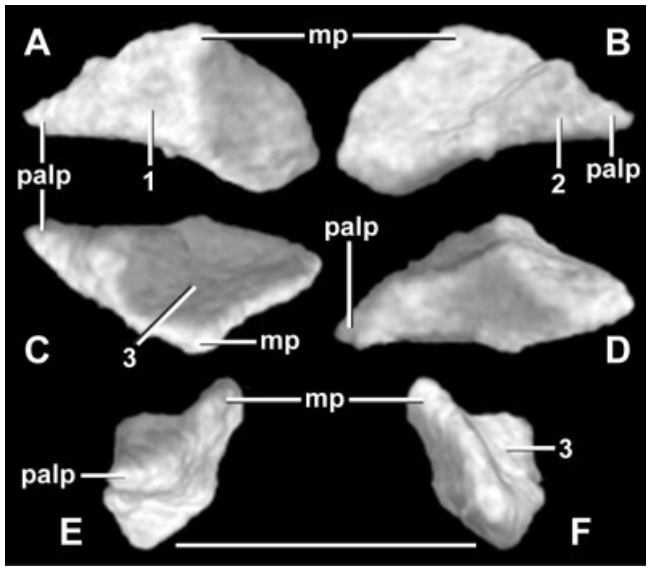

Fig. 12. Left ectopterygoid in (**A**) lateral, (**B**) medial, (**C**) dorsal, (**D**) ventral, (**E**) anterior, and (**F**) posterior views. Scale bar = 1 mm. mp, maxillary process; palp, palatine process; 1, surface of articulation with maxilla; 2, surface of articulation with palatine; 3, surface exposed in orbital floor.

The palatine is pierced by a single foramen, which penetrates the orbital lamina (Fig. 11A) near the anterior end of the articulation of the palatine with the pterygoid (Fig. 2D). It affords communication between the choanal vault and the temporal fossa, and carries the intermediate palatine branch of the facial nerve (VII) (Oelrich, 1956). There is no palatine foramen in *Rhineura* (Kearney et al., 2005) or *Amphisbaena* (Montero and Gans, 1999).

Ectopterygoid (Fig. 12; Tra 147–200). In *Diplometopon* the ectopterygoid is a paired element that lies between the maxilla and palatine along the lateral edge of the palate, where it also contributes to the floor of the orbit. The ectopterygoid contacts the maxilla along the anterior half of its length, and the palatine orbital lamina along its entire length. It gradually tapers to a point posteriorly. Its ventrolateral surface closely parallels the dorsomedial surface of the pterygoid palatine process (Tra 194).

The ectopterygoid is short, thick, and roughly triangular in cross section (Fig. 2C). A weak maxillary process (Fig. 12E) extends dorsolaterally to line the maxillary orbital process (Figs. 2C, 4B), and an even weaker palatine process (Fig. 12C) extends medially to meet the ventrolateral edge of the palatine orbital lamina (Tra 152). The simple morphology and articulations of the ectopterygoid in *Diplometopon* contrast sharply with those in *Rhineura* (Kearney et al., 2005) and *Amphisbaena* (Montero and Gans, 1999). In the latter taxa, the ectopterygoid bears an elongated, forked maxillary process that clasps the max-

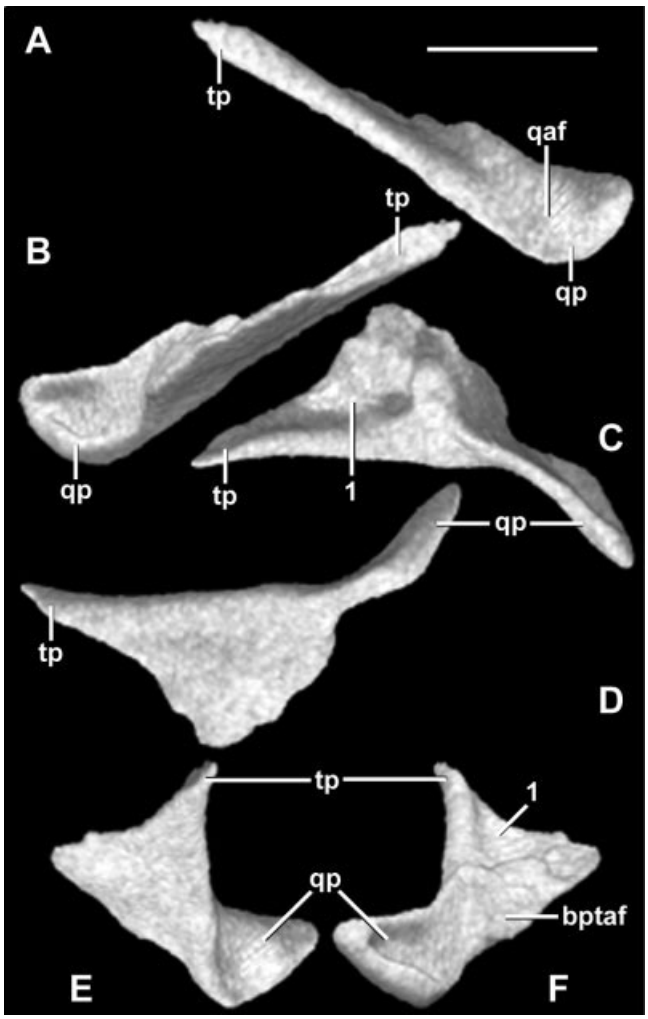

Fig. 13. Left pterygoid in (**A**) lateral, (**B**) medial, (**C**) dorsal, (**D**) ventral, (**E**) anterior, and (**F**) posterior views. Scale bar = 1 mm. bptaf, basipterygoid articular facet; qaf, quadrate articular facet; qp, quadrate process; tp, transverse process; 1, area of contact with palatine pterygoid process.

illary facial process and a robust forked pterygoid process that clasps the pterygoid transverse process.

Pterygoid (Fig. 13; Tra 187–327). The pterygoid is a paired element lying on either side of the midline of the ventral surface of the skull. In *Diplometopon* it articulates with the palatine anteriorly and with the parabasisphenoid and quadrate posteriorly. The pterygoids form the posteriormost portion of the palate. Each pterygoid is elongate and slightly concave dorsally. The parasagittal axis of the pterygoid is inclined anteriorly to parallel the sagittal crest of the skull, and emphasizes the angulation of the facial segment against the cranial segment (Fig. 13A).

The body of the pterygoid (=pterygoid plate of Montero and Gans, 1999) is a thin triangular plate that lies against the ventral surface of the palatine pterygoid process (Figs. 3B, 4C). Unlike in *Rhineura* (Kearney et al., 2005) and *Amphisbaena* (Montero and Gans, 1999), there is no anteromedial process that extends from the body to meet the vomer or palatine, respectively. Posteriorly, the body of the pterygoid lies in tight communication with the basipterygoid process (Fig. 2E) in a contact marked by a facet on the dorsomedial margin of the pterygoid (Fig. 13F).

The transverse process (=anterolateral process of Montero and Gans, 1999) (Fig. 13A) projects anterolaterally to lie along the edge of the palatine orbital lamina (Fig. 2D). The ectopterygoid briefly intervenes between the two anteriorly (Tra 194). Because of the close association of these three elements, the suborbital fenestra is closed (Fig. 5D; but see above). The transverse process exhibits more complex relationships in *Amphisbaena* (Montero and Gans, 1999), where it is clasped by the ectopterygoid pterygoid process, and especially in *Rhineura* (Kearney et al., 2005), where it interfingers with the ectopterygoid, maxilla, and palatine.

The quadrate process (=posterior process of Montero and Gans, 1999) (Fig. 13C) extends posterolaterally, forming a floor beneath an extracranial space known as the cavum epiptericum (Tra 265), which lodges the trigeminal (Gasserian) ganglion (Oelrich, 1956). The quadrate process turns laterally, closely approaching the mandibular compound bone (Fig. 2E) before abutting the quadrate (Fig. 3A). The area of contact with the quadrate is marked by a facet on the posterolateral surface of the quadrate process (Fig. 13A). The quadrate process continues further posteriorly, terminating in a blunt tip near the columellar shaft. The quadrate process exhibits similar relationships in *Rhineura* (Kearney et al., 2005) and *Amphisbaena* (Montero and Gans, 1999), but is not as distinctly developed in the latter.

Frontal (Fig. 14; Tra 082–207). The frontal is a complex, paired element in *Diplometopon*. It comprises two main divisions, the dorsal plate and the descending process, each with its own form and function. A similar configuration occurs in *Rhineura* (Kearney et al., 2005) and *Amphisbaena* (Montero and Gans, 1999). The superficial surface forms the leading surface or dorsal plate of the "spade snout" (Fig. 5E). The descending process lies beneath the dorsal plate and comprises two distinct laminae involved in forming the medial wall of the deeply sunken orbit and a tube that completely encircles the forebrain. The frontal is contacted by the premaxilla, nasal, and maxilla anteriorly, its counterpart medially, the orbitosphenoid ventrally and medially, and the parietal dorsally and posteriorly.

The dorsal plate (Fig. 14C) contacts the premaxilla, maxilla, nasal, and parietal. It forms the middle portion of the facial aspect of the skull, while also contributing to the roofs over the nasal chamber and the cranial cavity. The dorsal plate overhangs the orbit via a supraorbital ridge (Fig. 14A) that forms the orbital roof and contributes to the dorsal portion

of the orbital rim. The dorsal plate is gently convex, somewhat inclined toward the rostrum, and widest anterior to the orbit. The left and right frontals abut in a relatively straight suture along the medial surface of the dorsal plate (Fig. 2C), whereas they interdigitate in *Amphisbaena* (Montero and Gans, 1999) and *Rhineura* (Kearney et al., 2005).

Three fingers project anteriorly from the dorsal plate (Figs. 2B, 14C). The most medial finger, which is the broadest, wedges between the premaxillary nasal process and the nasal frontal process. The next most medial finger wedges between the nasal frontal process and the maxillary frontal process. The most lateral finger inserts into the bifurcate maxillary frontal process. The last is absent in *Amphisbaena* (Montero and Gans, 1999) and *Rhineura* (Kearney et al., 2005), both of which lack the bifurcate maxillary frontal process to receive it.

The posterior margin of the dorsal plate is also complex (Fig. 14C), exhibiting four major posteriorly projecting fingers that interdigitate with corresponding fingers on the anterior margin of the parietal (Fig. 5C). The dorsal plate also slightly overlaps the parietal (Fig. 3A), and this area of overlap is delimited by a shelf on the anterior margin of the parietal. This is also the case in *Rhineura* (Kearney et al., 2005), whereas in *Amphisbaena* (Montero and Gans, 1999) there is no overlap of the parietal by the frontal.

The dorsal plate lines the medial surface of the maxillary frontal process anterolaterally (e.g., Tra 130). The supraorbital ridge projects from the lateral margin of the dorsal plate posterior to the maxillary frontal process (Tra 148). It is almost immediately excluded from the dorsal margin of the orbit by an anteriorly projecting finger of the parietal (Tra 153). There is no finger-like supraorbital process in *Diplometopon*, unlike in *Amphisbaena* (=lateral process of Montero and Gans, 1999) and *Rhineura* (Kearney et al., 2005).

The surface of the dorsal plate is relatively smooth (Fig. 14C). It is pierced near its lateral edge by two communicating foramina that mark the endpoints of a frontal canal (Tra 132–155). A branch of the trigeminal ophthalmic nerve penetrates the dorsomedial wall of the orbit through the superior orbital foramen (Tra 157) (Fig. 14A) and feeds into this frontal canal. The condition in *Rhineura* is similar (Kearney et al., 2005), except that many more communicating foramina open into the surface of the dorsal plate. *Amphisbaena* is strikingly different

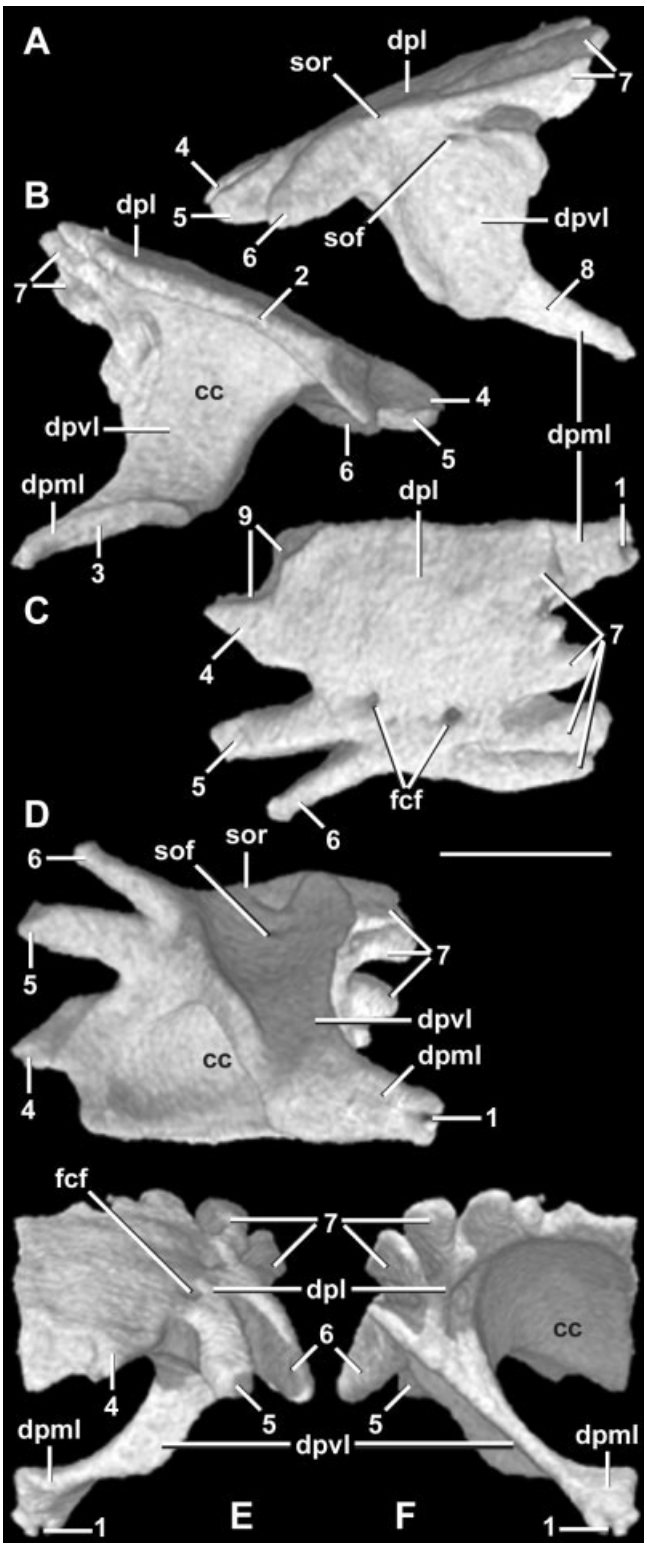

Fig. 14. Left frontal in (**A**) lateral, (**B**) medial, (**C**) dorsal, (**D**) ventral, (**E**) anterior, and (**F**) posterior views. Scale bar = 1 mm. cc, cranial cavity; dpl, dorsal plate; dpml, descending process medial lamina; dpvl, descending process vertical lamina; fcf, frontal communicating foramen; sof, superior orbital foramen; sor, supraorbital ridge; 1, notch that receives tip of parabasisphenoid orbitosphenoid process; 2, frontal-frontal contact (dorsal plates); 3, frontal-frontal contact (medial laminae of descending processes); 4, finger inserting between premaxilla and nasal; 5, finger inserting between nasal and maxilla; 6, finger inserting into maxillary frontal process; 7, fingers that articulate with parietal; 8, area underlain by orbitosphenoid; 9, area overlain by premaxillary nasal process.

(Montero and Gans, 1999) in that the frontal is completely unperforated and lacks a frontal canal.

The descending process (=ventral process and ventrolateral process of Montero and Gans, 1999) lies beneath the dorsal plate (Fig. 14A). It contacts the orbitosphenoid, parabasisphenoid, and parietal, but unlike in *Rhineura* (Kearney et al., 2005) and *Amphisbaena* (Montero and Gans, 1999), it does not contact the palatine. The descending process is organized around a vertical lamina of bone that descends ventromedially from the dorsal plate toward the floor of the orbit and braincase (Figs. 2C, 3A). The vertical lamina is inclined posteriorly and gradually turns to form an anteroposteriorly broadened medial lamina (Fig. 14A). The medial lamina exhibits a notch on its posterior margin (Fig. 14F) that receives the anterior tip of the parabasisphenoid orbitosphenoid process (Fig. 3A). As in *Amphisbaena* (Montero and Gans, 1999), the descending process lacks a temporal wing. The condition in *Rhineura* (Kearney et al., 2005) is markedly different, with a pronounced temporal wing projecting posteriorly to form part of the lateral wall of the braincase.

The vertical lamina forms the medial wall of the orbit as it descends from beneath the dorsal plate (Tra 156). It is penetrated near its junction with the dorsal plate by the superior orbital foramen (Tra 158) (Fig. 14A), which transmits cutaneous innervation and vasculature to the posterior surface of the dorsal plate. This is also the case in *Rhineura* (Kearney et al., 2005).

The vertical lamina also forms the long lateral wall of the anterior part of the cranial cavity (Figs. 3B, 14B). The base of this wall curves inward as the medial lamina, which projects to contact its counterpart along the ventral midline, thereby forming a floor beneath the cranial cavity (Fig. 2C). Thus, the frontals form a complete and robust bony tube that encircles the forebrain, an unusual condition that is present throughout amphisbaenians (Zangerl, 1944; Vanzolini, 1951) and in some other squamates such as snakes. No perforations in this tubular forebrain housing are apparent in *Diplometopon*. Additionally, the cranial cavity is open anteriorly (Fig. 14E) via the olfactory fenestra (=frontal fenestra of Montero and Gans, 1999), which provides a large passageway for the neuronal axons of the olfactory epithelium of the nasal chamber.

The medial laminae are underlain posteriorly by the orbitosphenoid anteromedial process (Tra 158) (Fig. 3C). The orbitosphenoid anterolateral processes begin to line the lateral walls of the cranial cavity further posteriorly, at the level of the widest point of the supraorbital ridge (Tra 170) (Fig. 2C). The orbitosphenoid anteromedial and anterolateral processes merge near the level of the frontoparietal suture (Tra 180), at which point the cranial cavity is lined by the orbitosphenoid laterally, the frontal descending processes ventrally, and the parietal dorsally. The descending processes terminate just posterior to the anterior tips of the parabasisphenoid orbitosphenoid processes (Tra 207), leaving the parietal, parabasisphenoid, and orbitosphenoid to close the cranial cavity (Fig. 2D). These relationships are quite different in *Rhineura* (Kearney et al., 2005), where paired orbitosphenoids lie dorsal to the medial laminae, completely enclosed within the braincase.

Parietal (Fig. 15; Tra 152–419). The parietal is unpaired in *Diplometopon*, but it may have developed from paired ossification centers that fused early in ontogeny as in *Amphisbaena darwini* (Montero et al., 1999). The parietal is a domed element that is constricted at the narrowest point of the skull, just behind the frontoparietal suture (Fig. 5C). The anterodorsal surface of the parietal contributes a large triangular portion to the deflected facial segment of the skull. The apical process (Figs. 3C, 15B) forms the tallest prominence of the skull, at the point of deflection between the facial and cranial segments. A midline sagittal crest arises just behind the apical process and extends posteriorly along the entire length of the bone. Its development in *Diplometopon* and *Rhineura* (Kearney et al., 2005) is weak relative to *Amphisbaena* (Montero and Gans, 1999), where the sagittal crest reaches a height almost one-third the total height of the parietal. As in other amphisbaenians, there is no pineal foramen. The parietal forms most of the roof and anterolateral walls of the cranial cavity.

The parietal contacts the frontal anterodorsally in a complex suture (Fig. 5C). Three major lateral fingers (e.g., Tra 173) and several minor medial fingers (e.g., Tra 189) project anteriorly from the parietal to interdigitate with corresponding fingers on the posterior margins of the frontal dorsal plates. The anterolateral process of the parietal comprises the three lateral fingers (Figs. 2C, 15A). The anterior margin of the parietal is overlain slightly by posterior projections of the frontal dorsal plates (Fig. 3A,B), resulting in a weakly developed shelf (Fig. 15B).

The temporal lamina (=lateral plate of Montero and Gans, 1999) (Fig. 15A) descends from the skull roof to form much of the external surface of the anterior braincase (Figs. 2D, 3A). Its ventral edge contacts the orbitosphenoid anteroventrally (Fig. 3A), the parabasisphenoid ventrally (Fig. 4B), and the alar process (=anterolateral process of Montero and Gans, 1999) posteriorly (Fig. 4A). The temporal lamina contributes to the anterodorsal margin of the Gasserian foramen (Fig. 4B). This is also the case in *Amphisbaena* (Montero and Gans, 1999), whereas in *Rhineura* (Kearney et al., 2005) it is excluded from this margin by the prootic alar process. These areas of contact are delimited by shallow shelves on the ventral and posterolateral surfaces of the temporal lamina (Fig. 15A,C).

The parietal broadly overlies the roof of the vestibular chamber of the otic–occipital complex (Fig.

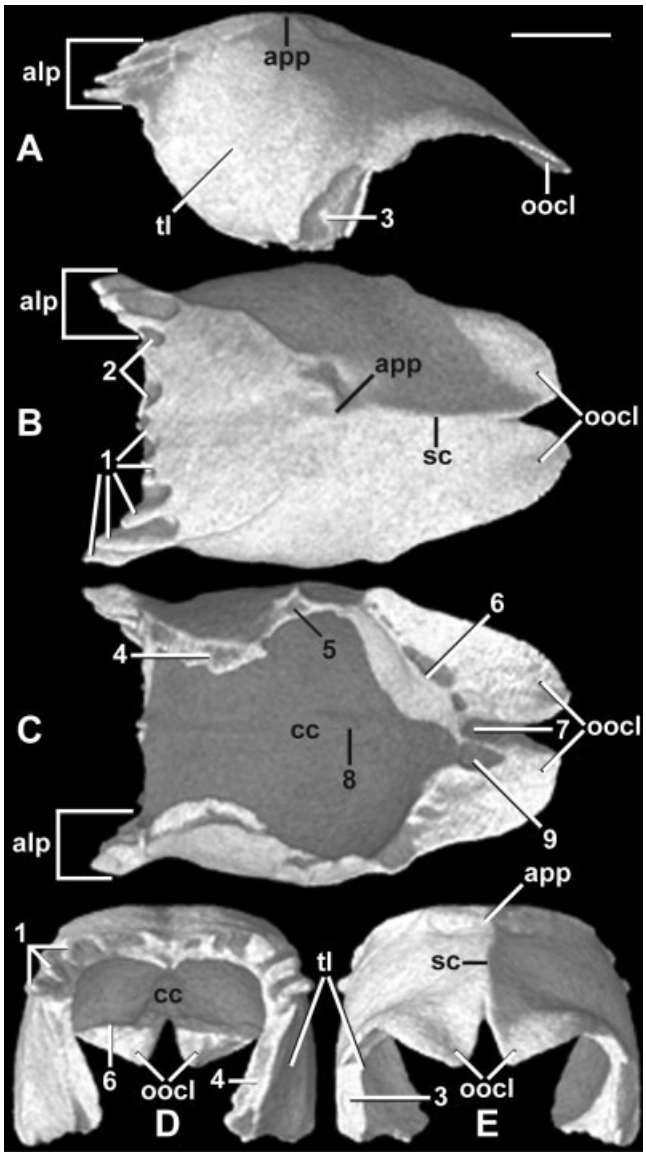

Fig. 15. Parietal in (**A**) lateral, (**B**) dorsal, (**C**) ventral, (**D**) anterior, and (**E**) posterior views. Anterior to left in **A–C**. Scale bar = 1 mm. alp, anterolateral process; app, apical process; cc, cranial cavity; oocl, otic–occipital lappet; sc, sagittal crest; tl, temporal lamina; 1, fingers inserting into notches on posterior margin of frontal dorsal plate; 2, areas of overlap by posterior fingers of frontal; 3, area of overlap by prootic alar process; 4, area of overlap by orbitosphenoid; 5, area of overlap by parabasisphenoid; 6, ridge delimiting overlap of otic–occipital complex; 7, channel receiving supraoccipital ascending process; 8, sulcus reflecting sagittal crest; 9, depression marking dorsalmost point of anterior verticular semicircular canal.

2F). As in amphisbaenians generally, there is no posttemporal fenestra and no supratemporal process of the parietal. A channel on the posteroventral surface of the parietal (Fig. 15C) receives the supraoccipital ascending process (Fig. 2G), which extends anteriorly to approximately the midpoint of the otic capsule (Fig. 3B). The parietal divides smoothly just anterior to the origin of the supraoccipital ascending process into bilateral lappets (=posterior plates of Montero and Gans, 1999) that overlie the supraoccipital (Figs. 2H, 3A, 15B). The posterior margins of the lappets are bluntly rounded (Fig. 15B) and lie well anterior to the supraoccipital occipital crest (Fig. 5C).

The central vault of the internal surface of the parietal is relatively smooth (Fig. 15C), except for a shallow sulcus reflecting the position of the sagittal crest (Fig. 2E). A pronounced ridge marks the point where the parietal begins to overlie the otic–occipital complex (Fig. 15C). Bilateral depressions immediately posterior to this ridge mark the dorsalmost point of the anterior verticular semicircular canals (Figs. 2F, 3A).

Otic–occipital complex and squamosal (Figs. 2–4, 16; Tra 193–441). In *Diplometopon*, the separate embryonic ossifications of the otic and occipital units become conjoined above and below the foramen magnum, creating the fused otic–occipital complex. As in *Rhineura* (Kearney et al., 2005), the parabasisphenoid and squamosal are also coosified with the otic–occipital complex. These bones are figured and described as a single unit below. For convenience of more general comparisons among squamates, the constituent parts are then described region-by-region. Lastly, the internal morphology of the endocranium and otic capsule is summarized from front to back as viewed in successive HRXCT slices (Figs. 2–4).

External Anatomy of Otic–Occipital Complex (Fig. 16). In lateral view (Fig. 16A), the otic–occipital complex inclines from its shallowest anterior point at the cultriform process tip (Tra 193) to its deepest posterior point (Tra 356), where "Element X" (Zangerl, 1944) caps the ventrolateral process. The parabasiphenoid forms the anteriormost and median portion of the basicranium (Fig. 16E), while the cranial cavity is bounded laterally by the otic complex and dorsally and posteriorly by the occipital complex. The jugular recess is largely obscured from view, as in *Amphisbaena* (Montero and Gans, 1999), whereas it is fully exposed laterally in *Rhineura* (Kearney et al., 2005).

In posterior view (Fig. 16B), the paroccipital process marks the widest point of the otic–occipital complex, where the horizontal semicircular canal reaches its greatest lateral inflection. The cranial cavity is restricted dorsally by the medial inflection of the otic capsules. The margins of the foramen magnum are formed by the occipital complex dorsally and ventrally and the otic capsules laterally. The border of the foramen magnum is roughly triangular in shape, with the occipital crest rising prominently above it. The occipital condyle is U-shaped, expanding upwards around the ventral portion of the foramen magnum. This differs from the dumbbell-shaped condyle in *Rhineura* (Kearney et al., 2005) and the bicipital condyle in *Amphisbaena* (Montero and Gans, 1999). These differences

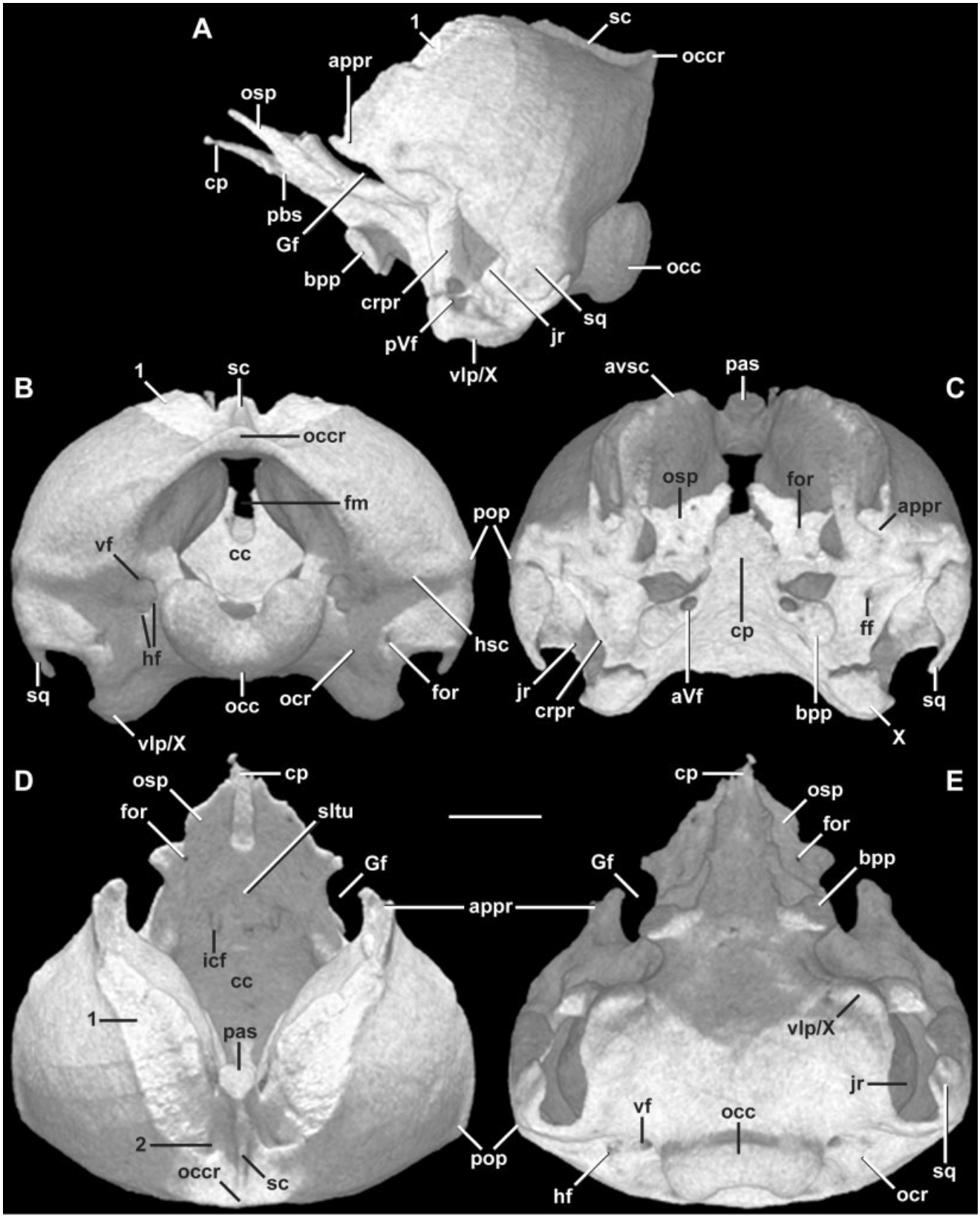

Fig. 16. Otic–occipital complex and squamosal in (**A**) lateral, (**B**) posterior, (**C**) anterior, (**D**) dorsal, and (**E**) ventral views. Anterior up in **D,E**. Scale bar = 1 mm. appr, alar process of prootic; aVf, anterior Vidian foramen; avsc, anterior vertical semicircular canal; bpp, basipterygoid process; cc, cranial cavity; cp, cultriform process of parabasisphenoid; crpr, crista prootica; ff, facial foramen; fm, foramen magnum; for, foramen; Gf, Gasserian foramen; hf, hypoglossal foramen; hsc, horizontal semicircular canal; icf, internal carotid foramen; jr, jugular recess; occ, occipital condyle; occr, occipital crest; ocr, occipital recess; osp, orbitosphenoid process of parabasisphenoid; pas, processus ascendens of supraoccipital; pbs, parabasisphenoid; pop, paroccipital process; pVf, posterior Vidian foramen; sc, sagittal crest; sltu, sella turcica; sq, squamosal; vf, vagus foramen; vlp, ventrolateral process; X, "element X"; 1, area of overlap by parietal lappet; 2, depression receiving parietal descending finger.

presumably relate to different head postures during stereotyped digging behaviors among "spade-headed," "shovel-headed," and "round-headed" amphisbaenians (Gans, 1974). The occipital recess houses four foramina: the vagus foramen dorsally; two hypoglossal foramina medially; and another foramen laterally that communicates with the perilymphatic duct.

In anterior view (Fig. 16C), the otic–occipital complex is roughly oval. Its dorsal surface rises to an apex that is formed by the supraoccipital processus ascendens and the dorsalmost limit of the anterior verticular semicircular canal. The cranial cavity, although open at the olfactory fenestra, is mostly obscured from view by the dorsally inclined parabasisphenoid. The anterior Vidian foramen lies at the medial corner of the basipterygoid process (Tra 279), which is much more protuberant than in *Rhineura* (Kearney et al., 2005) or *Amphisbaena* (Montero and Gans, 1999). The facial foramen penetrates the otic–occipital complex anteromedial to the crista prootica. The jugular recess is partially obscured in this view by the pronounced crista prootica medially and the squamosal laterally.

In dorsal view (Fig. 16D), the prootic alar processes extend anteriorly to the level of the sella turcica. The otic capsules extend dorsomedially to form the beginnings of the endocranial roof. The otic–occipital complex is roofed posteriorly by the supraoccipital, which completely obscures the occipital condyle. This differs from the condition in *Rhineura* (Kearney et al., 2005) and *Amphisbaena* (Montero and Gans, 1999), where the occipital condyle is visible in dorsal view. The sagittal crest, which is continued forward in the articulated specimen as the sagittal crest of the parietal, projects along the dorsal midline of the supraoccipital. A moderately well-developed occipital crest runs along the posterodorsal margin of the supraoccipital. This crest is also prominent in *Amphisbaena* (Montero and Gans, 1999), but apparently absent in *Rhineura* (Kearney et al., 2005). The supraoccipital processus ascendens, which extends from the anterior end of the sagittal crest, fits into a median channel on the parietal. A shallow depression on either side of the processus ascendens receives a small descending finger of the parietal (Tra 402). This relationship is also present in *Rhineura* (Kearney et al., 2005) but not in *Amphisbaena* (Montero and Gans, 1999). The dorsomedial margin of the otic capsule exhibits a shallow excavation that marks the area of overlap by each parietal lappet. The otic capsules are smooth and bulbous and form most of the dorsal surface of the otic–occipital complex. The internal carotid foramen pierces the parabasisphenoid at the posterolateral edge of the sella turcica. Anterolateral to this, a small foramen pierces the parabasisphenoid orbitosphenoid process.

In ventral view (Fig. 16E), the otic–occipital complex is roughly triangular, with the anterior tip of the cultriform process forming the apex of the triangle and the otic capsules forming its corners. The prootic alar process extends anteriorly lateral to the parabasisphenoid, arching above the Gasserian foramen that is visible between these two elements. The pronounced basipterygoid process is located at the level of the Gasserian foramen and is oriented anterolaterally. This is also its orientation in *Amphisbaena* (Montero and Gans, 1999), whereas in *Rhineura* it faces directly anteriorly (Kearney et al., 2005). The ventrolateral process, capped by "Element X," lies further posteriorly. The voluminous otic capsules lie behind the basipterygoid processes, and the occipital complex closes the cranial cavity posteriorly.

Parabasisphenoid Complex. In *Diplometopon*, the parasphenoid and basisphenoid are coosified to form the parabasisphenoid, which in turn is partially coossified with the basioccipital. Thus, the boundaries between these elements can only be estimated. The parabasisphenoid exhibits three anterior processes (Figs. 2D, 4B, 16E): a median cultriform process and dorsolateral orbitosphenoid processes. The cultriform process extends over approximately the anterior third of the otic–occipital complex (Fig. 16E). The basipterygoid process lies at one-third the distance between the tip of the cultriform process and the occipital condyle, and the protuberant ventrolateral process lies approximately midway between the basipterygoid process and the occipital condyle.

The anterior tip of the cultriform process inserts into the space formed between the palatines and the body of the orbitosphenoid (Figs. 2D, 4B). This is also the case in *Amphisbaena* (Montero and Gans, 1999), whereas in *Rhineura* (Kearney et al., 2005) it inserts into the space between the frontal descending processes, palatines, and vomers. The cultriform process broadens posteriorly to the base of the basipterygoid process (Tra 269) (Fig. 16E).

The orbitosphenoid process lies dorsal and lateral to the cultriform process (Fig. 16C), inserting into a shallow depression on the dorsal surface of the orbitosphenoid (Fig. 2D). The orbitosphenoid process flares posterolaterally to form the anterior margin of the Gasserian foramen (Fig. 4B). Near its widest point, the orbitosphenoid process is pierced at midbody by a small foramen (Fig. 16D) that also penetrates the underlying orbitosphenoid (Tra 252). The orbitosphenoid process contacts the parietal temporal lamina laterally just anterior to the Gasserian foramen (Tra 248), thereby excluding the orbitosphenoid from the braincase wall in this region.

The anterior floor of the cranial cavity is formed by the dorsal surface of the parabasisphenoid (Fig. 16D). The sella turcica, which lodges the pituitary gland, is a shallow basin in the dorsal surface of the parabasisphenoid at the level of the basipterygoid process (Fig. 2E). The internal carotid foramen opens into the cranial cavity through the floor of the sella turcica.

The basipterygoid process protrudes sharply beneath the Gasserian foramen (Figs. 2E, 16E), extending anterolaterally to articulate with the pterygoid. It is relatively constricted at the base and flares distally into a broad, flat, anteroventrally oriented articular surface (Fig. 2E). The ventrolateral process swells behind the basipterygoid process (Figs. 3B, 16C). It is capped by "Element X" (Zangerl, 1944), the homology of which is problematic (Lakjer, 1927; Zangerl, 1944; Vanzolini, 1951; Kesteven, 1957; Jollie, 1960; Gans, 1960, 1978). In this specimen of *Diplometopon*, "Element X" is mostly coosified with the ventrolateral process, although sutures are readily apparent anteriorly (Fig. 16C). It is composed of spongy bone, as is the case in *Rhineura* (Kearney et al., 2005) and *Amphisbaena* (Montero and Gans, 1999).

Otic Complex. The embryonic otic capsule, which ossifies as separate prootic and opisthotic bones in other squamates, coosifies in amphisbaenians along with the rudimentary squamosal (when present) and "Element X" to form a single fused otic complex (Zangerl, 1944; Kesteven, 1957; Montero et al., 1999). The quadrate and columella articulate with the otic complex.

The otic complex is conjoined to the occipital complex above and below the foramen magnum (Fig. 16B). The supraoccipital forms the roof of the cranial cavity and unites the right and left otic capsules dorsally. The exoccipital is confluent with the posteroventral wall of the otic capsule ventrolateral to the foramen magnum.

The short prootic alar process contributes to the lateral closure of the braincase (Figs. 4B, 16A). Its anterior tip lies ventral to the parietal temporal lamina (Fig. 4B), whereas posteriorly it overlaps the parietal temporal lamina laterally (Fig. 2E); this area of overlap is delimited by a ridge on the ventrolateral surface of the parietal temporal lamina. The ventral margin of the alar process forms the dorsal and posterior borders of the Gasserian foramen (Fig. 4B). This is also the case in *Amphisbaena* (Montero and Gans, 1999), whereas in *Rhineura* (Kearney et al., 2005) it also forms the anterior border of the Gasserian foramen. The combined root of the trigeminal nerve (V) passes from the cranial cavity through this opening into the cavum epiptericum (e.g., Tra 267). There it balloons into the Gasserian (trigeminal) ganglion and divides into the ophthalmic (V_1), maxillary (V_2), and mandibular (V_3) branches of the trigeminal nerve (Oelrich, 1956).

The otic capsule is a voluminous spherical chamber that dominates the back of the skull (Fig. 16D). A large jugular recess is excavated into the capsule beneath the horizontal semicircular canal (Figs. 2G, 16A), opening laterally. The dorsal edge of the jugular recess is bounded by the paroccipital process (Fig. 2G), its anterior edge is formed by the crista prootica (Fig. 16A), and its posterior edge is formed by the crista tuberalis. Its external aspect is partially bounded by the squamosal (Fig. 2G).

The facial foramen pierces the prootic just anterior to the crista prootica (Figs. 4C, 16C) where the trunk of cranial nerve VII exits the cranial wall. The posterior Vidian foramen occurs at the junction of the crista prootica and the ventrolateral process (Figs. 2F, 16A), then opens into the Vidian canal (=parabasal canal of Montero and Gans, 1999) (Fig. 2E). The canal conveys the internal carotid artery and palatine branch of the facial nerve (VII) longitudinally through the parabasisphenoid until opening beneath the sella turcica (deBeer, 1937; Oelrich, 1956; Jollie, 1960). The canal continues its anterior course and emerges into the cavum epiptericum through the anterior Vidian foramen, which is located at the base of the basipterygoid process (Figs. 3A, 16C). The fenestra ovale opens ventrolaterally into the jugular recess slightly medial to the paroccipital process (Fig. 2G). The footplate of the columella is enormous and completely fills the fenestra ovale.

The occipital recess is an excavation between the crista tuberalis and the occipital condyle (Figs. 4C, 16B). Four foramina open into the occipital recess. The most ventral foramen pierces the anterolateral wall of the occipital recess (Fig. 3A) and communicates with the perilymphatic duct (Tra 398). The other three foramina are clustered at the dorsal apex of the occipital recess (Fig. 16B). The vagus foramen is dorsalmost (Fig. 4C) and transmits the glossopharyngeal (IX) and vagus (X) nerve trunks and the internal jugular vein. Two smaller hypoglossal foramina, occurring just below the vagus foramen (Tra 408) (Fig. 16B), transmit branches of the hypoglossal nerve (XII). The vagus and hypoglossal foramina follow direct routes from the cranial cavity as they pierce the cranial wall. In *Amphisbaena*, the occipital recess apparently houses only one large foramen identified as the vagus (Montero and Gans, 1999). One foramen is also present in *Rhineura*; however, the HRXCT data show it to be a combined opening for distinct vagus and hypoglossal passages (Kearney et al., 2005).

Occipital Complex. The supraoccipital, paired exoccipital, and basioccipital coosify to form the occipital complex in amphisbaenians (Montero et al., 1999). As in other reptiles, the basioccipital contributes to the floor of the braincase, the exoccipital to its walls, and the supraoccipital to its roof.

In *Diplometopon*, the basioccipital portion of the occipital complex forms the most posterior portion of the braincase floor between the otic capsules as well as the median portion of the occipital condyle. The dorsal surface of the basioccipital is smooth and forms an arched floor beneath the hindbrain (Fig. 3C). The supraoccipital portion of the occipital complex forms the roof of the foramen magnum, the posterior part of the braincase, and the dorsal portion of the otic complex. The foramen magnum opens

posteriorly and is not elevated (Fig. 3C). Looking into the foramen magnum (Fig. 16B), the dorsal portion of the cranial cavity is largely filled by the projecting dorsomedial walls of the otic capsules.

Squamosal. The squamosal is coossified with the otic–occipital complex in *Diplometopon* (Fig. 16A) such that its margins are discernable only in section (e.g., Tra 339) and, even then, only anteriorly. It forms a roughly rectangular tab that extends ventrally from the posteroventral corner of the otic capsule (Fig. 16A), covering the columellar footplate posteriorly (Fig. 2G) and terminating at the level of the midpoint of the columellar shaft (Sag 037). The squamosal contributes to the posteroventral portion of the articular surface for the quadrate cephalic condyle (Fig. 4C). The squamosal is globular proximally, but dramatically thins and elongates into a platelike structure distally (Fig. 2G).

The position of the squamosal is strikingly displaced ventrally in *Diplometopon* relative to the typical squamate condition. A squamosal was not identified in *Diplometopon* by Gans (1960); however, he figured a similar platelike structure partially covering the columellar footplate in several trogonophid species. El-Assy and Al-Nassar (1976) identified a topologically equivalent element in *Diplometopon* as the supratemporal; however, its significant contribution to the quadrate articulation suggests that it is the squamosal. A coossified squamosal was identified in *Rhineura* (Kearney et al., 2005) but not in *Amphisbaena* (Montero and Gans, 1999).

Internal Anatomy of Otic–Occipital Complex (Figs. 2–4). The internal morphology of the endocranium and the otic capsule are described, in turn, from anterior to posterior with reference to representative HRXCT sections.

Anteriorly (Tra 158), the cranial cavity is roughly heart-shaped and almost completely enclosed by the frontals, with a small contribution from the orbitosphenoid anteromedial process. More posteriorly (Fig. 2C), the orbitosphenoid anterolateral processes begin to form the lateral walls of the cranial cavity. They eventually meet the orbitosphenoid anteromedial process, thereby excluding the frontal descending processes from the lateral wall (Tra 183). At this point, the parietal anterolateral processes begin to exclude the frontal from the dorsal margin of the cranial cavity. At the posterior limit of the frontal descending processes (Tra 205), the parabasisphenoid orbitosphenoid processes begin to contribute to the floor of the cranial cavity and the parietal forms its dorsal and lateral walls (Fig. 2D). Eventually, the parabasisphenoid orbitosphenoid processes contact the parietal temporal laminae (Tra 227), thereby excluding the orbitosphenoid from all but the ventromedial tip of the cranial cavity (Fig. 4B). Further posteriorly (Tra 233), the parabasisphenoid orbitosphenoid and cultriform processes converge and the orbitosphenoid posteromedial process terminates (Tra 242) (Fig. 3C). At this point the shape of the cranial cavity is circular.

The Gasserian foramen opens between the parietal temporal lamina and parabasisphenoid (Tra 255). The prootic alar process begins to contribute to the dorsal border of the Gasserian foramen at approximately the same level that the orbitosphenoid posterolateral process terminates (Tra 265) (Fig. 4B). Just posterior to this (Tra 277), the anterior Vidian foramina pierce the parabasisphenoid at the proximal corners of the basipterygoid processes (Fig. 3A). The internal carotid canal opens into the floor of the cranial cavity (Fig. 2E) just anterior to the closure of the Gasserian foramen (Tra 288). Further posteriorly, the prootic meets the parabasisphenoid to close the Gasserian foramen (Tra 297) (Fig. 4C).

Expansion of the otic capsules begins to constrict the cranial cavity posterior to the level of the Gasserian foramen (Tra 313) (Fig. 4B). The facial foramina exit the endocranial cavity near the anterodorsal margin of the crista prootica posterior to the basipterygoid processes (Tra 318) (Fig. 4C). The anterior auditory foramina pierce the endocranial cavity from the vestibules of the otic capsules (Tra 324). The Vidian canals exit through the posterior Vidian foramina at the suture of the parabasisphenoid, prootic, and "Element X" (Tra 330) (Fig. 2F). Posterior to this, the cranial cavity becomes further constricted dorsally due to great enlargement of the vestibules (Tra 345). The posterior auditory foramina enter the cranial cavity from the ventromedial corners of the vestibules (Tra 350) (Fig. 3B). Constriction of the cranial cavity reaches its greatest development at the widest point of the otic–occipital complex (Fig. 2G), at which point the endolymphatic canals enter the cranial cavity from the dorsomedial walls of the vestibules (Fig. 4A).

Near the level of the posterior margin of the fenestrae ovali (Fig. 2H), the recessus scalae tympani mark the entrance of the perilymphatic ducts into the ventrolateral corners of the cranial cavity. Further posteriorly (Tra 406), the vagus foramina exit the cranial cavity (Fig. 3B) and travel ventrolaterally to open into the occipital recesses (Fig. 4C). The hypoglossal foramina do the same slightly further posteriorly (Tra 410).

Moving back to the anterior end of the otic complex, the anterior vertical semicircular canal opens at a level near the midpoint of the Gasserian foramen (Tra 285). It emerges from the anterior ampullary recess and abruptly arcs posterodorsally (Fig. 4B) to eventually meet the recessus crus communis (Figs. 2H, 3B). The vestibule opens just posterior to the anterior ampullary recess (Tra 301) (Fig. 3A). The statolithic mass then appears and the horizontal semicircular canal emerges laterally from the anterior ampullary recess (Tra 314). The statolithic mass is an ovoid calcified body that expands posteriorly to fill roughly half of the vestibule (Fig. 4B). Further posteriorly, the anterior auditory foramen

exits the vestibule (Tra 324) and the perilymphatic duct differentiates from the ventral margin of the vestibule (Tra 328) (Fig. 2F). This duct runs for almost the entire length of the otic capsule, eventually opening into the dorsal aspect of the recessus scalae tympani (Tra 385) (Fig. 2G). Throughout its length the perilymphatic duct is open to the lagenar recess, which begins near the level of the anterior margin of the fenestra ovale (Tra 341).

The fenestra ovale begins to open at the level of the origin of the ventrolateral processes (Tra 339). The posterior auditory foramen then opens into the cranial cavity from the vestibule (Fig. 3B). Continuing posteriorly, the perilymphatic duct opens into the recessus scalae tympani (Tra 385) and the anterior vertical semicircular canal opens into the recessus crus communis (Figs. 2H, 3B). The recessus scalae tympani then opens into the cranial cavity via the medial aperture (Fig. 2H) and the posterior vertical semicircular canal emerges from the recessus crus communis (Tra 394) (Fig. 3B).

The fenestra ovale closes and the lagenar recess ends just anterior to the occipital recess (Tra 401). The horizontal and posterior semicircular canals enter the posterior ampullary recess at the level of the vagus and hypoglossal canals (Figs. 3A, 4C).

Orbitosphenoid (Fig. 17; Tra 150–267). The orbitosphenoids are fused in many amphisbaenians (=tabulosphenoid of Montero and Gans, 1999), greatly enlarged, and possibly augmented by a dermal component (Zangerl, 1944; Bellairs and Gans, 1983; Montero et al., 1999). In *Diplometopon*, as in *Amphisbaena* (Montero and Gans, 1999), the orbitosphenoid is platelike and lies in close apposition with the frontal descending processes. In *Rhineura* (Kearney et al., 2005) the paired orbitosphenoids lie dorsal to the frontal descending processes and are hidden from external view. The orbitosphenoid in *Diplometopon* is butterfly-shaped (Fig. 17B), with the body paralleling the angulation of the cranial segment and the wings more steeply inclined anteriorly (Fig. 17A). It contacts the frontals anterodorsally and dorsolaterally, the parietal dorsally, and the parabasisphenoid posterodorsally and posteroventrally.

The orbitosphenoid exhibits three anterior processes (Fig. 17B). The anteromedial process inserts into the space between the palatines and the frontal descending processes (Figs. 2C, 3C); its ventral surface is marked by a ridge that extends posteriorly approximately half the length of the orbitosphenoid (Fig. 17C). The anterolateral processes line the medial surfaces of the frontal descending processes (Fig. 2C), and this area of overlap is delimited by a ridge on the ventral surface of the anterolateral process (Fig. 17A). The anterolateral processes meet the anteromedial process (Fig. 2D) to fully enclose the posterior edges of the frontal descending processes (Fig. 4A). A pronounced ridge on the dorsomedial surface of the orbitosphenoid delimits the

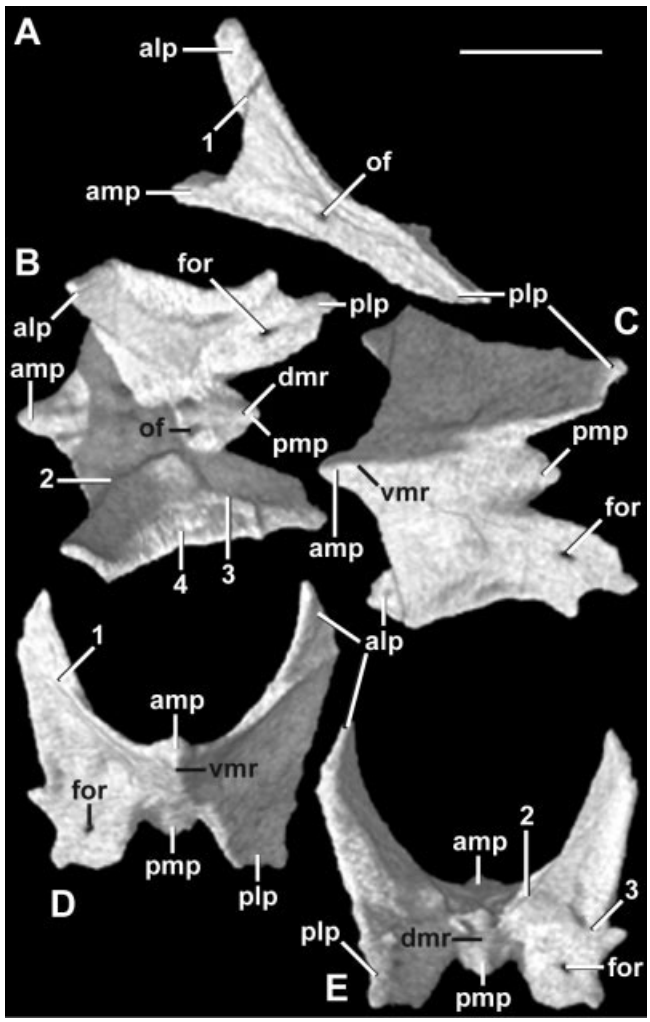

Fig. 17. Orbitosphenoid in (**A**) lateral, (**B**) dorsal, (**C**) ventral, (**D**) anterior, and (**E**) posterior views. Anterior to left in **A–C.** Scale bar = 1 mm. alp, anterolateral process; amp, anteromedial process; dmr, dorsomedial ridge; for, foramen; of, optic foramen; plp, posterolateral process; pmp, posteromedial process; vmr, ventromedial ridge; 1, ridge delimiting area of overlap by frontal descending process; 2, ridge delimiting area of overlap of frontal descending process; 3, ridge delimiting area of overlap of parabasisphenoid orbitosphenoid process; 4, area of contact with parietal temporal lamina.

area of overlap of the frontal (Fig. 17B). The orbitosphenoid in *Amphisbaena* (Montero and Gans, 1999) exhibits only anterolateral processes that line the ventral aspect of the frontal descending processes, and is completely excluded from the walls of the cranial cavity by the frontals.

The orbitosphenoid in *Diplometopon* also exhibits three posterior processes (Fig. 17B). The posteromedial process is clasped by the parabasisphenoid orbitosphenoid processes (Tra 233) (Fig. 3B); its surface exhibits a dorsomedial ridge that extends anteriorly half the length of the orbitosphenoid (Fig. 17B). The posterolateral processes line the ventrolateral surfaces of the parabasisphenoid orbitosphe-

noid processes (Fig. 4B); the extent of this contact is delimited by a ridge on the ventral surfaces of the latter and on the dorsal surfaces of the former (Fig. 17B). The lateral edge of the orbitosphenoid contacts the ventral edge of the parietal temporal lamina (Fig. 2D), and a longitudinal shelf marks this contact (Fig. 17B). The orbitosphenoid contributes to the closure of the ventrolateral braincase wall (Figs. 2D, 4A) before terminating at the level of the midpoint of the Gasserian foramen. The orbitosphenoid in *Amphisbaena* (Montero and Gans, 1999) lacks a posteromedial process; this margin of the orbitosphenoid interdigitates with the parabasisphenoid.

The orbitosphenoid is pierced by two sets of laterally paired foramina. The optic foramen (Figs. 2D, 17A) occurs at midbody and opens into the cranial cavity, providing passage for the optic nerve. It has a similar position in *Amphisbaena* (Montero and Gans, 1999) but is absent in *Rhineura* (Kearney et al., 2005). A smaller foramen, centered in the orbitosphenoid posterolateral process (Tra 238) (Fig. 17C), also pierces the overlying parabasisphenoid to enter the cranial cavity.

Quadrate (Fig. 18; Tra 278–359). The quadrate in *Diplometopon* is short and stout, its lateral aspect obscured by the extracolumella distally. The shaft is narrower than the slightly expanded distal mandibular condyle and the greatly expanded proximal cephalic condyle (Fig. 18A). The shaft is less dramatically constricted in *Rhineura* (Kearney et al., 2005) and *Amphisbaena* (Montero and Gans, 1999). The quadrate in *Diplometopon* reclines at an angle of almost 45° relative to the long axis of the skull, similar to the orientation in *Rhineura* (Kearney et al., 2005), but steeper than that in *Amphisbaena* (30°; Montero and Gans, 1999). The pterygoid quadrate process in *Diplometopon* extends posteroventrally to lie in apposition with the medial surface of the mandibular condyle (Fig. 3A). The mandibular condyle gently clasps the pterygoid quadrate process in *Amphisbaena* (Montero and Gans, 1999), whereas in *Rhineura* (Kearney et al., 2005) the reverse is true.

The posteroventral margin of the quadrate in *Diplometopon* is deeply concave (Fig. 18A) to allow passage of the stout columellar shaft from the jugular recess to the extracolumella. The columellar shaft is comparatively more slender in *Amphisbaena* (Montero and Gans, 1999) and *Rhineura* (Kearney et al., 2005), and its passage from the jugular recess is accommodated by a notch on the relatively straight posterior aspect of the quadrate shaft. Each quadrate in *Diplometopon* exhibits one or more irregularly placed nutritive foramina (Fig. 18C,F), as in *Rhineura* (Kearney et al., 2005) and *Amphisbaena* (Montero and Gans, 1999). *Amphisbaena* also possesses a relatively large lateral foramen (Montero and Gans, 1999) that penetrates the cephalic condyle lateromedially.

The cephalic condyle in *Diplometopon* articulates simply with the squamosal/paroccipital process posterodorsally (Figs. 2F, 4C), as in *Rhineura* (Kearney et al., 2005). In *Amphisbaena* (Montero and Gans, 1999), the cephalic condyle is augmented by an extension (lateral plate) that wraps around the paroccipital process, creating an almost ball-and-socket joint. In *Diplometopon*, the mandibular condyle forms a saddle-shaped articulation with the mandibular glenoid fossa anteroventrally (Figs. 2E, 3A). The two condyles are oriented perpendicular to each other (Fig. 18E), with the long axis of the cephalic condyle positioned vertically and that of the mandibular condyle positioned horizontally. The dorsal crest is a vertical ridge that runs along the anterolateral edge of the quadrate between the two condyles. The cephalic condyle is anteroposteriorly expanded, with a pronounced posteroventral process (Fig. 18A) that extends over the dorsal surface of the columellar shaft to abut the platelike squamosal ventral process (Fig. 4C).

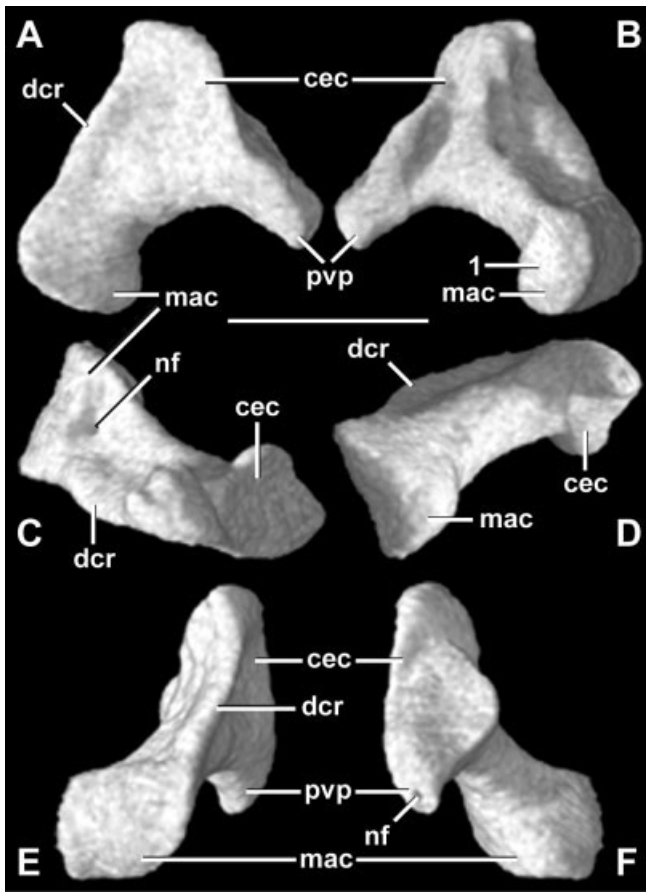

Fig. 18. Left quadrate in (**A**) lateral, (**B**) medial, (**C**) dorsal, (**D**) ventral, (**E**) anterior, and (**F**) posterior views. Scale bar = 1 mm. cec, cephalic condyle; dcr, dorsal crest; mac, mandibular condyle; nf, nutritive foramen; pvp, posteroventral process; 1, surface of articulation with pterygoid.

Columella (Fig. 19; Tra 315–400) and extracolumella (Fig. 20; Tra 243–322). The columella in *Diplometopon* consists of a short shaft that expands proximally into a basal footplate. An enlarged, min-

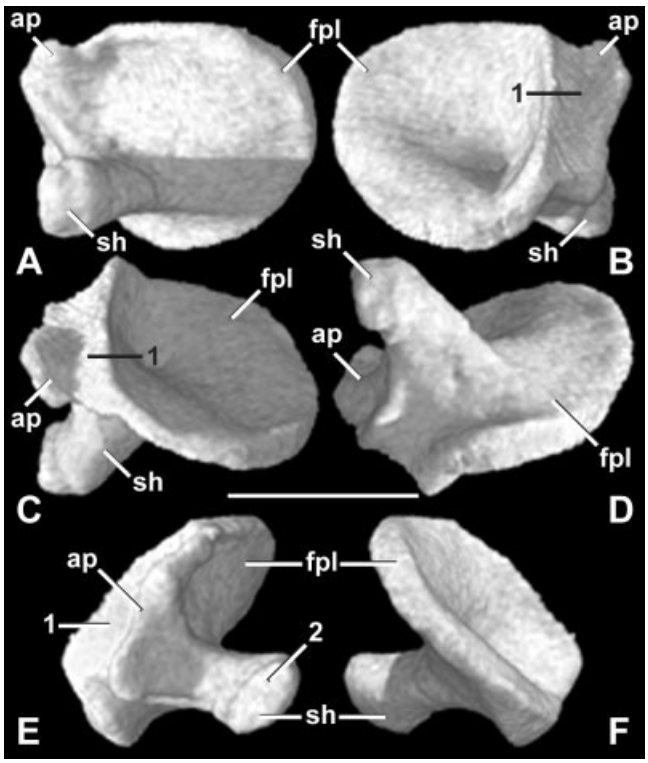

Fig. 19. Left columella in (**A**) lateral, (**B**) medial, (**C**) dorsal, (**D**) ventral, (**E**) anterior, and (**F**) posterior views. Scale bar = 1 mm. ap, anterior process; fpl, footplate; sh, shaft; 1, trough receiving crista prootica; 2, extracolumellar attachment surface.

eralized, fan-shaped extracolumella extends anteriorly from the distal tip of the columella almost to the level of the coronoid process (Fig. 5A).

The basal footplate is proportionally huge, subcircular (Fig. 19A), and laterally inclined (Fig. 19E), fitting into the deeply recessed fenestra ovale (Fig. 2G). Its external surface is smooth (Fig. 19A). The footplate expands both anteriorly and medially to form an anterior process (Fig. 19C) that lacks an analog in *Amphisbaena* (Montero and Gans, 1999) and *Rhineura* (Kearney et al., 2005). This anterior process clasps the crista prootica (Figs. 3A, 4C), and this contact is delimited by a trough running along its dorsomedial aspect (Fig. 19B). The medial surface of the footplate is deeply concave, unlike in *Rhineura* (Kearney et al., 2005) and *Amphisbaena* (*contra* Montero and Gans, 1999). The center of the medial surface of the footplate is pierced by a foramen (Tra 352) that does not occur in *Rhineura* (Kearney et al., 2005) or *Amphisbaena* (Montero and Gans, 1999).

A short, robust shaft arises from the lateral face of the columellar footplate anteroventral to its center (Fig. 19A). It is roughly circular in cross-section, as in *Rhineura* (Kearney et al., 2005), whereas in *Amphisbaena* (Montero and Gans, 1999) it is dorsoventrally compressed. In *Diplometopon*, the columellar shaft extends anterolaterally under the quadrate cephalic condyle (Fig. 2F), terminating in a rounded knob (Fig. 19E) that attaches to the extracolumella.

In amphisbaenians, the extracolumella may be absent, present and cartilaginous, or present and partially or fully mineralized (Kearney, 2003). In most trogonophid amphisbaenians the extracolumella is enlarged, platelike, and fully mineralized (Gans, 1960), which is the case in *Diplometopon*. The extracolumella in *Amphisbaena* is mineralized, slender, and rod-like, extending anteriorly just past the apex of the coronoid process (Montero and Gans, 1999). This element was not preserved in *Rhineura hatcherii* (Kearney et al., 2005), but it is described as short and mineralized in the extant *R. floridana* (Gans, 1978).

The extracolumella in *Diplometopon* is dorsoventrally expanded anteriorly (Fig. 20A). Its medial surface is gently concave (Fig. 20E) and lies in close apposition with the quadrate mandibular condyle (Fig. 2E). The extracolumella terminates posteriorly in a flat surface (Fig. 20F) that articulates with the columellar shaft (Tra 321).

Overview of Mandible (Fig. 21)

The lower jaw in *Diplometopon* consists of two rami joined anteriorly in a symphyseal articulation and articulating posteriorly with the quadrates.

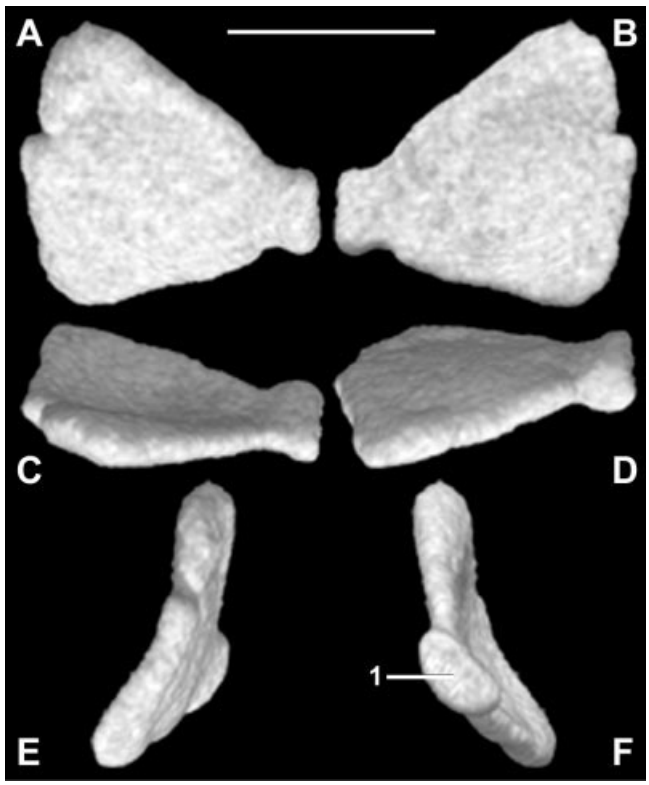

Fig. 20. Left extracolumella in (**A**) lateral, (**B**) medial, (**C**) dorsal, (**D**) ventral, (**E**) anterior, and (**F**) posterior views. Scale bar = 1 mm. 1, columellar attachment surface.

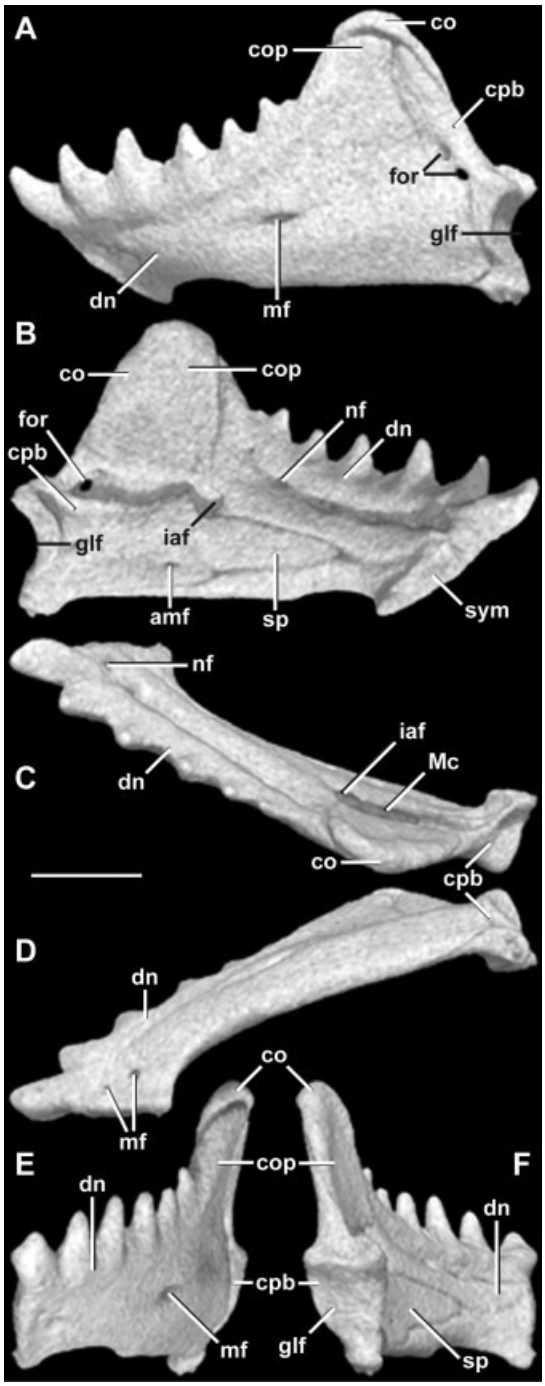

Fig. 21. Right mandible (inverted) in (**A**) labial, (**B**) lingual, (**C**) dorsal, (**D**) ventral, (**E**) anterior, and (**F**) posterior views. Scale bar = 1 mm. amf, anterior mylohyoid foramen; co, coronoid; cop, coronoid process; cpb, compound bone; dn, dentary; for, foramen; glf, glenoid fossa; iaf, inferior alveolar foramen; Mc, Meckelian canal; mf, mental foramen; nf, nutritive foramen; sp, splenial; sym, symphyseal articular surface.

Each ramus curves anteromedially to meet its opposite in a deep, flat symphyseal surface (Tra 092) (Fig. 21B). A shallow, posteriorly facing, C-shaped glenoid fossa (Figs. 3A, 21F) receives the quadrate mandibular condyle, which has an anterolateral orientation. The postdentary elements are extremely reduced, and there is no retroarticular process.

The mandible exhibits two mental foramina near its anterior end (Tra 098, 112) (Fig. 3C) and one at midbody (Tra 184) (Figs. 3A, 21A). The Meckelian canal is closed along most of its length, its walls formed by the dentary labially and the splenial lingually (Fig. 2C). The canal is open at its anterior end (Tra 146) (Fig. 21A), and then briefly opens dorsally (Tra 202–235) (Figs. 2D, 21C) before exiting via the anterior mylohyoid foramen (Tra 263) (Fig. 21B). A dentary canal runs through the dentary below the tooth row (Fig. 2B), exiting through the inferior alveolar foramen at the point of dorsal exposure of the Meckelian canal (Figs. 3A, 21B). The posterior end of the mandible is pierced by two foramina (Tra 255, 264) (Fig. 21A), one of which may be the posterior mandibular foramen (see Compound bone, below).

In most amphisbaenians, the postdentary elements exhibit significant fusion, resulting in a compound postdentary bone. Gans (1960) interpreted the mandible of *Diplometopon* to comprise dentary, coronoid, angular, surangular, prearticular, and articular. Only three discrete mandibular elements can be identified confidently in the specimen studied here: dentary, coronoid, and compound bone (Fig. 21A). *Contra* Gans (1960), we interpret the anterior projection of the compound bone to represent a coosified splenial (Fig. 21B) based on its lingual exposure and closure of the Meckelian canal (Fig. 2C). It is not possible to determine what other elements are present in the compound bone without developmental studies.

The mandible is short (approximately half the total length of the skull) and very deep (approximately half the maximum height of the skull), with a pronounced coronoid process that extends dorsally to the level of the orbit (Fig. 5A). The mandibular coronoid process is formed by the coronoid, with a major contribution from the dentary coronoid process and a minor contribution from the compound bone (Figs. 4B, 21A).

Individual Elements of Mandible

Dentary (Fig. 22; Tra 054–278). The dentary in *Diplometopon* bears six acrodont teeth along its dorsal margin (Fig. 22A), in contrast to the seven subpleurodont teeth in *Rhineura* (Kearney et al., 2005) and the eight in *Amphisbaena* (Montero and Gans, 1999). The first tooth is the largest in *Diplometopon*, with tooth size generally diminishing towards the back of the tooth row. The bases of the teeth are bulbous, hollow (Fig. 4C) and fused to each other, and some give the impression of having small accessory cusps (Fig. 22A). A small subdental shelf extends medial to the tooth row just posterior to the first tooth (Figs. 2C, 22C). Nutritive foramina are

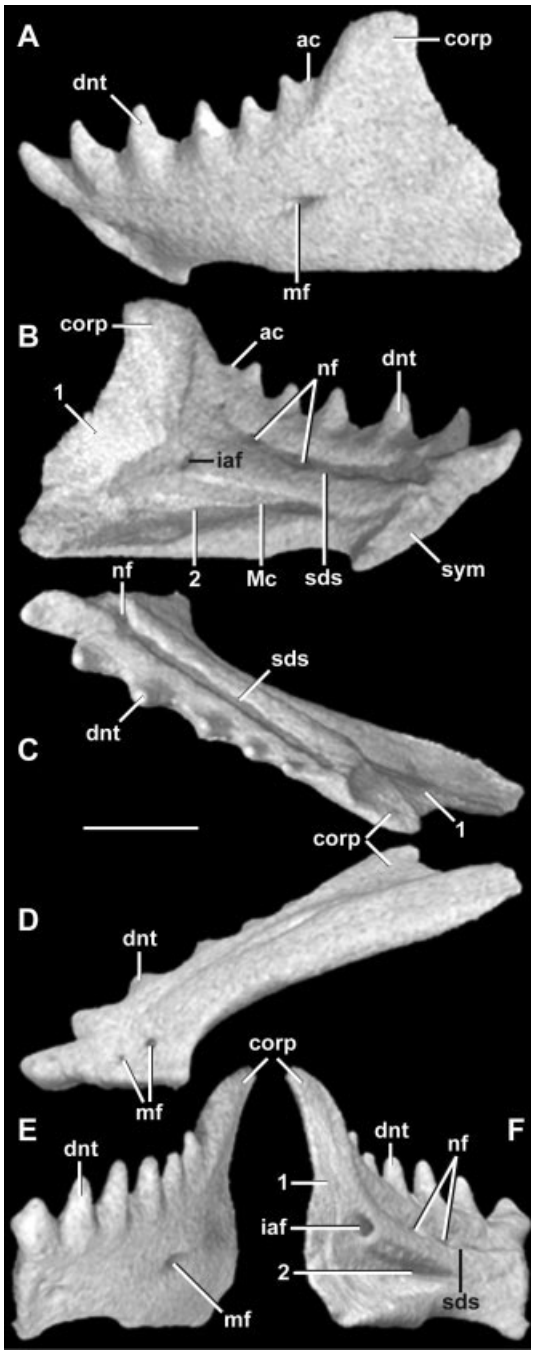

Fig. 22. Right dentary (inverted) in (**A**) labial, (**B**) lingual, (**C**) dorsal, (**D**) ventral, (**E**) anterior, and (**F**) posterior views. Scale bar = 1 mm. ac, accessory cusp; corp, coronoid process; dnt, dentary tooth; iaf, inferior alveolar foramen; Mc, Meckelian canal; mf, mental foramen; nf, nutritive foramen; sds, subdental shelf; sym, symphyseal articular surface; 1, area of overlap by coronoid and compound bones; 2, area of overlap by splenial.

present along the subdental shelf at the base of each tooth (Figs. 3B, 22B).

A small dentary canal (Fig. 2B,C) runs the length of the dentary, transmitting the inferior alveolar nerve and artery. It communicates with the three mental foramina on the labial surface of the dentary (Figs. 3A, 22A) and gives off a nutritive foramen to the base of each tooth (Fig. 3B). It exits posteriorly through the inferior alveolar foramen at the level of the anterior edge of the coronoid process (Figs. 3A, 22F). The Meckelian canal is expressed as a posteriorly widening groove on the lower aspect of the lingual surface of the dentary (Fig. 22B). In the articulated mandible, the canal is open anteriorly, originating at the level of the third tooth (Tra 145). It is closed lingually halfway between the third and fourth tooth (Tra 150) by the splenial portion of the compound bone (Figs. 2C, 3B). Posteriorly, the canal is open dorsally (Figs. 2D, 3A, 21C) from the level of the inferior alveolar foramen (Tra 201) to the level of the apex of the coronoid bone (Tra 238). This opening appears to correspond to the "central foramen" of Montero and Gans (1999).

The symphyseal surface at the anterior end of the dentary is vertically oriented and slightly broader dorsally than ventrally (Figs. 2B, 22B). It is sharply pointed ventrally, more so than in *Amphisbaena* (Montero and Gans, 1999) and *Rhineura* (Kearney et al., 2005). The ventral margin of the dentary is gently concave posteriorly to the level of the fourth tooth, then straight thereafter (Fig. 22A).

A pronounced coronoid process (=posterodorsal process of Montero and Gans, 1999) projects dorsally from just behind the last dentary tooth (Fig. 22A). The dentary coronoid process is mediolaterally compressed (Figs. 2D, 22F) and lies in apposition with the coronoid and compound bones medially (Fig. 4B) and the coronoid dorsally (Tra 224). This is also the case in *Amphisbaena* (Montero and Gans, 1999), whereas in *Rhineura* (Kearney et al., 2005) the dentary coronoid process is relatively tiny and is clasped by the coronoid dorsally.

The posterior margin of the dentary in *Diplometopon* lacks distinct processes. It slopes steeply from the coronoid process (Fig. 22A) to lie in simple apposition with the lateral surface of the compound bone (Fig. 4C), and this contact is delimited by a ridge on the posterior margin of the latter. The posterior margin of the dentary in *Amphisbaena* (Montero and Gans, 1999) exhibits a posteroventral process that articulates with the compound bone dorsally. In *Rhineura* (Kearney et al., 2005), an articular process lies along the labial surface of the compound bone, and a ventral process clasps the ventral margins of the splenial and compound bones.

Coronoid (Fig. 23; Tra 203–264). The coronoid in *Diplometopon* is a simple, small element that forms the dorsalmost edge of the mandibular coronoid process (Figs. 4A, 5A). The coronoid in amphisbaenians may be extensively overlapped by a large dentary coronoid process, slightly overlapped by a small process, or not overlapped at all (Kearney, 2003); the first is the condition in trogonophids.

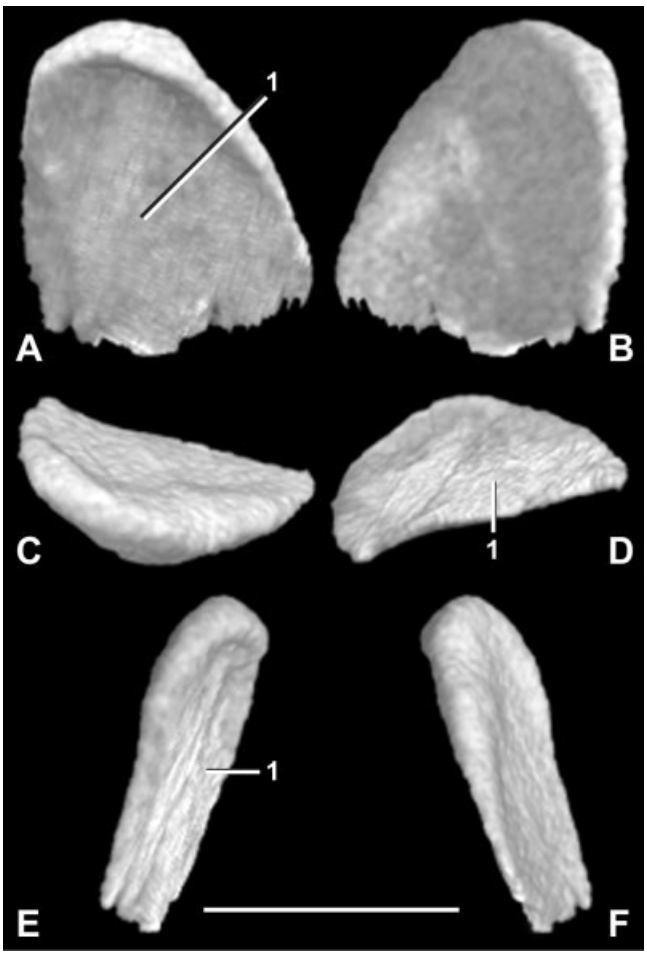

Fig. 23. Right coronoid bone (inverted) in (**A**) labial, (**B**) lingual, (**C**) dorsal, (**D**) ventral, (**E**) anterior, and (**F**) posterior views. Scale bar = 1 mm. 1, area of overlap by dentary and compound bone.

The coronoid is an inverted parabola in lateral view (Fig. 23A) with the long axis anteriorly inclined. It is strongly mediolaterally compressed with a thickened dorsal edge (Figs. 2D, 23E). It lies in apposition to the medial surface of the dentary coronoid process and the compound bone (Tra 234) (Fig. 4B), and curves laterally above these elements to form the dorsal and posterior edge of the mandibular coronoid process. The coronoid extends ventrally (Fig. 23B) almost to the level of the inferior alveolar foramen (Fig. 2D), thinning significantly towards its ventral margin. The coronoid is much more complex in *Rhineura* (Kearney et al., 2005), with anterior processes that clasp the dentary coronoid process and a posterior process that lines the lingual surface of the compound bone to the anterior margin of the posterior mandibular foramen. In *Amphisbaena* (Montero and Gans, 1999), the coronoid briefly clasps the dorsal margin of the compound bone and extends posteriorly, as in *Rhineura*. In all three taxa the coronoid covers most of the lingual surface of the mandibular coronoid process.

Compound bone (Fig. 24; Tra 148–300). The compound postdentary bone presumably incorporates the fused supraangular, articular, prearticular, and splenial in most amphisbaenians (Montero

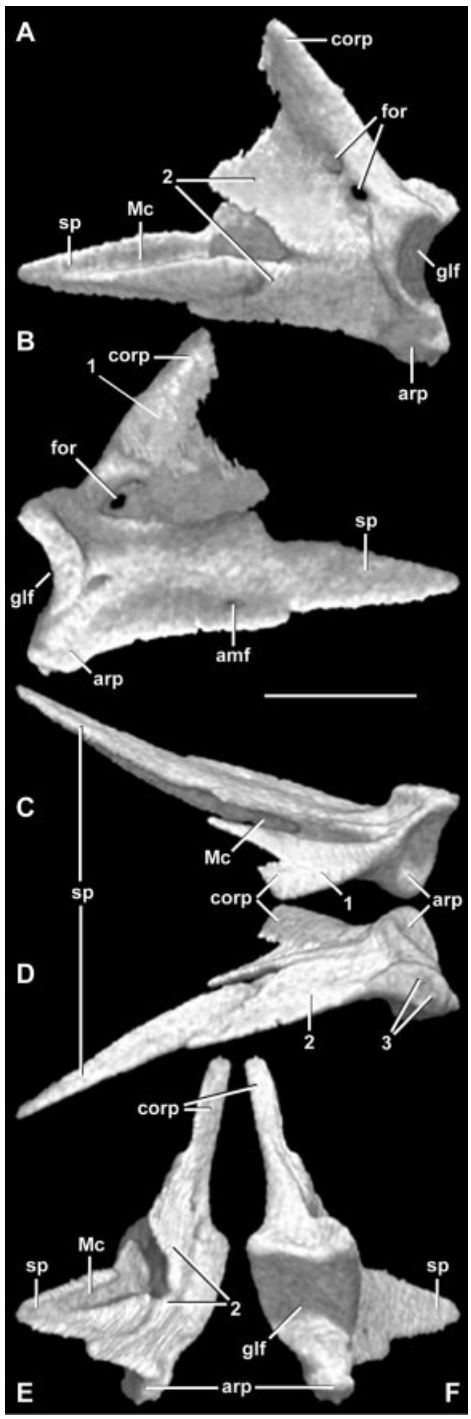

Fig. 24. Right compound bone (inverted) in (**A**) labial, (**B**) lingual, (**C**) dorsal, (**D**) ventral, (**E**) anterior, and (**F**) posterior views. Scale bar = 1 mm. amf, anterior mylohyoid foramen; arp, articular process; corp, coronoid process; for, foramen; glf, glenoid fossa; Mc, Meckelian canal; sp, splenial; 1, area of overlap by coronoid; 2, area of overlap by dentary; 3, ventral projections.

and Gans, 1999; Montero et al., 1999). Most of these elements are indistinguishable in *Diplometopon* due to fusion. However, based on the topological relationships discussed above, we interpret the anterior projection of the compound bone to be the coosified splenial (Fig. 24A).

The compound bone is the most posterior component of the mandible. It is a triradiate element (Fig. 24A), exhibiting an anterior projection (the coossified splenial), a dorsal coronoid process, and a posterior articular process. The compound bone contacts the dentary, coronoid, quadrate, and pterygoid.

The splenial is a thin, flattened bony projection lying along a groove in the dentary and located entirely on the medial surface of the mandible (Fig. 2C,D). It forms the lingual wall of the Meckelian canal (Fig. 24E). It is exposed along its entire length, extending anteriorly and tapering to a point just past the midpoint of the fourth dentary tooth (Tra 150). The posterior extent of the splenial cannot be determined due to its coosification with the compound bone. However, a small foramen that we interpret to be a reduced anterior mylohyoid foramen (Fig. 24B) occurs at the level of the anterior edge of the coronoid process (Tra 265). This suggests that the splenial extends posteriorly at least this distance into the compound bone. The anterior mylohyoid foramen transmits the anterior mylohyoid nerve (Oelrich, 1956).

The bladelike coronoid process extends anterodorsally (Fig. 24A) to contribute to the mandibular coronoid process (Fig. 4B). In the articulated mandible, its superior portion is exposed in lateral view (Fig. 21A), but obscured in medial view by the coronoid (Fig. 21B). Its inferior portion is largely obscured, sandwiched between the dentary coronoid process labially and the coronoid lingually (Fig. 4B). A small portion is visible ventral to the coronoid medially (Fig. 24B). A deep sulcus at the base of the coronoid process represents the open portion of the Meckelian canal (Fig. 24B,C). The coronoid process in *Amphisbaena* (Montero and Gans, 1999) is fully exposed labially, but mostly obscured lingually by the coronoid. The compound bone in *Rhineura* (Kearney et al., 2005) lacks a coronoid process.

Two foramina pierce the compound bone near the base of the coronoid process (Fig. 24A). The ventral one (Tra 264) is slightly larger than the dorsal one (Tra 258), and both follow a direct path from the labial to the lingual surface. These foramina communicate with the Meckelian canal, which is open in this region (Fig. 3A). Based on their position and pathway, one of them probably represents the posterior mandibular foramen.

The articular process comprises a shallow, C-shaped glenoid fossa (Figs. 3A, 24A) that is oriented posterolaterally (Fig. 24F) to receive the anteromedially oriented quadrate mandibular condyle (Fig. 2E). The anteromedial portion of the articular process loosely contacts the pterygoid quadrate process, whereas the former tightly clasps the latter in *Amphisbaena* (Montero and Gans, 1999) and *Rhineura* (Kearney et al., 2005). The articular process extends ventrally into a short, robust knob (Fig. 24D), the ventral surface of which exhibits two small projections. There is no retroarticular process, as in *Amphisbaena* (Montero and Gans, 1999) but not *Rhineura* (Kearney et al., 2005). Numerous nutritive canals occur within the articular process (Fig. 2E) in all three taxa.

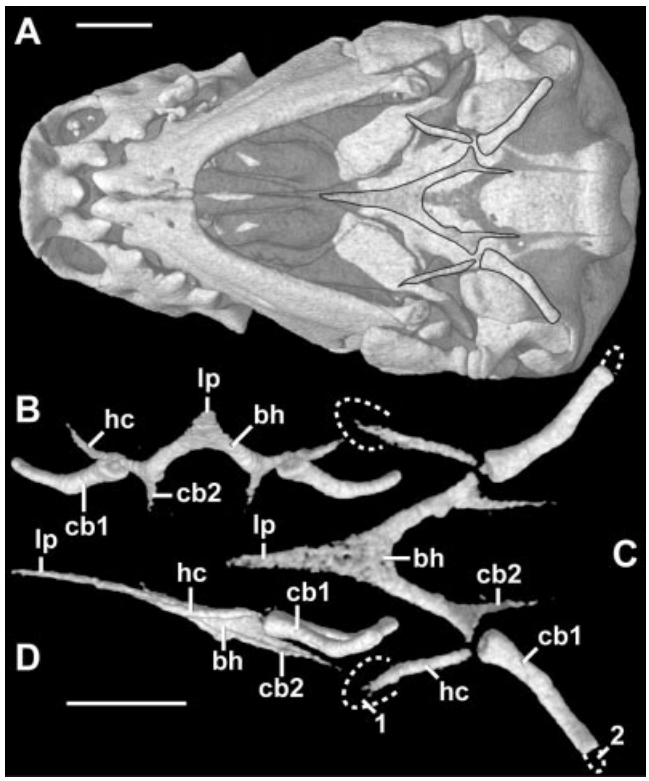

Fig. 25. Hyobranchial apparatus in (**A**) ventral view with skull showing natural position, edges outlined for clarity, (**B**) anterior, (**C**) dorsal, and (**D**) lateral views. Scale bars = 1 mm. bh, basihyal; cb1, first ceratobranchial; cb2, second ceratobranchial; hc, hyoid cornu; lp, lingual process; 1, area expanded by cartilaginous paddle-shaped tip; 2, area extended by cartilaginous first epibranchial.

Hyobranchial Apparatus (Fig. 25; Tra 217–391)

The hyobranchial apparatus consists of cartilaginous and mineralized elements that serve as the skeletal support for the tongue and throat. Although the hyobranchium of *Diplometopon* has been figured previously (Gans, 1960; El-Assy and Al-Nassar, 1976), for completeness we include a description here as it is part of the head skeleton. Only those portions of the hyobranchium that are mineralized can be seen in HRXCT data, thus we augment our

description with examination of a cleared-and-stained specimen. The hyobranchium in *Amphisbaena* was not described by Montero and Gans (1999), and was not preserved in *Rhineura* (Kearney et al., 2005).

The hyobranchium in *Diplometopon* lies along the ventral aspect of the skull, extending from the pyriform recess anteriorly to approximately the occipital condyle posteriorly (Fig. 25A). At its widest point it extends just past the jugular recess. The hyobranchium as a whole is gently inclined anteriorly (Fig. 25D), such that its anterior half is obscured by the mandible in the articulated skull in lateral view (Fig. 5A). The hyobranchium comprises the basihyal, lingual process, first and second ceratobranchials, hyoid cornua (anterior processes), and first epibranchials (Fig. 25C). The first epibranchials and the connection between the hyoid cornua and the basihyal are not visible in the HRXCT data because they lack mineralization.

The basihyal is the central element of the hyobranchium. It is an inverted U-shaped element whose center lies between the basipterygoid processes and the ventrolateral processes of the otic–occipital complex (Fig. 25A). The posterior arms of the basihyal flare slightly at their distal ends. This element is completely mineralized in mature *Diplometopon* (Fig. 25C). The lingual process arises from the anterior apex of the basihyal, gradually tapering to a point at the level of the pyriform recess (Fig. 25A). It is mostly mineralized and there is no visible discontinuity between it and the basihyal. The second ceratobranchials arise from the posterior arms of the basihyal (Fig. 25C). These extend posteriorly almost to the posterior margin of the ventrolateral processes (Fig. 25A), gradually tapering to a point. The second ceratobranchials are moderately well-mineralized and exhibit no visible discontinuity with the basihyal (Fig. 25C).

Two elements articulate with each posterior arm of the basihyal (Fig. 25A). The hyoid cornu extends anterolaterally to closely approach the posteroventral edge of the mandible. It is a mineralized rod proximally, while distally it expands into a cartilaginous, flattened, paddle-shaped tip (Fig. 25C) near the level of the apex of the basihyal. The first ceratobranchial extends posterolaterally from the posterior arm of the basihyal to the posterior portion of the jugular recess (Fig. 25A). It exhibits a distinct dorsolateral bend at its midpoint (Fig. 25B,D) and is thicker proximally than distally (Fig. 25C). As in squamates generally, the first ceratobranchial is hollow (Fig. 2F) and is the only hyobranchial element to truly ossify. The cartilaginous first epibranchial arises from the distal tip of the first ceratobranchial (Fig. 25C) and extends to the posterolateral edge of the skull.

DISCUSSION

Historically, amphisbaenian taxonomy reflected multiple rationales, including morphology, function, and biogeography (e.g., Vanzolini, 1951; Gans, 1974, 1978). The emergence of phylogenetic systematics initiated a search for shared derived characters as the basis for inferring phylogeny. Recent phylogenetic studies (Kearney, 2003; Kearney and Stuart, 2004) support the recognition of five monophyletic amphisbaenian lineages that differ somewhat in content and diagnosis from the groupings derived from pre-phylogenetic methods. Resolution of phylogenetic relationships remains somewhat poor, however, partially due to the incongruence between morphology-based and molecular-based approaches. Additionally, at least part of the problem in resolving the relationships among these five lineages is lack of morphological data and concomitant difficulties in assessing homology for phylogenetic character coding.

Those amphisbaenian species that have now been described in detail (*Amphisbaena alba*, *Rhineura hatcherii*, and *Diplometopon zarudnyi*) begin to allow a more refined assessment of the homology of structures. For example, both *Diplometopon* and *Rhineura* have a strong craniofacial angulation and a rostral digging blade that are related to use of the head in burrowing, but these features are built in different ways. In *Diplometopon*, the facial segment of the skull is foreshortened and flattened, forming a straight line from its point of deflection to the tip of the snout, whereas in *Rhineura*, the facial segment is elongated and its surface is smoothly rounded. Elongated nasals and an elongated premaxillary nasal process contribute to approximately half the length of the facial segment of the skull in *Diplometopon*, while in *Rhineura* the nasals are relatively short and elongated frontals comprise at least half of the facial segment. Additionally, *Rhineura* exhibits an extraordinary degree of sculpturing and perforating canals on the facial bones, indicating a high degree of sensory innervation; these structures are mostly absent in *Diplometopon*. In *Rhineura*, a well-developed maxillary nasal process projects anteriorly to clasp the nasal rostral process. The former is reduced to a miniscule spine in *Diplometopon*, thus there is no contribution from the maxilla to the rostral blade. These comparisons do not support hypotheses of homology relative to the spatulate heads in these taxa.

Discovery of cranial elements not detectable before the availability of HRXCT data will also affect future phylogenetic studies. In the morphological data matrix of Kearney (2003), several characters related to internal cranial morphology were scored as "?" for *Diplometopon* due to the inability to observe them clearly on scarce museum specimens. These characters can now be scored based on the HRXCT data provided here. For example, the dis-

covery of the splenial and squamosal in *Diplometopon* and *Rhineura* will change character codings which may, in turn, affect phylogenetic hypotheses.

These studies also reveal a major distinction between the closure of the anterior braincase in *Rhineura, Diplometopon*, and *Amphisbaena*. A large, platelike orbitosphenoid forming the anterolateral wall of the braincase has traditionally been considered a uniquely diagnostic character for amphisbaenians (Gans, 1978; Bellairs and Gans, 1983). This element is thought to represent the fusion of primitively paired orbitosphenoids augmented by a dermal component, and this is the condition in both the "spade-headed" *Diplometopon* and the "round-headed" *Amphisbaena*. However, in the "shovel-headed" *Rhineura*, the orbitosphenoids are small, paired elements that are completely enclosed within the braincase; the anterolateral braincase wall is closed instead by a large temporal wing of the frontal (Kearney et al., 2005). A similar condition reportedly occurs in the "shovel-headed" amphisbaenid *Monopeltis capensis* (Kritzinger, 1946). Thus, the closure of the braincase is achieved differently in different amphisbaenian lineages. Whether the conditions in *Rhineura* and *Monopeltis* are homologous, and whether the single orbitosphenoid seen in *Amphisbaena* and *Diplometopon* represents the primitive or derived condition for amphisbaenians, remains unclear in the absence of a stable phylogenetic hypothesis. However, observations such as these will aid in homology assessment and the accurate construction and coding of phylogenetic characters in future analyses.

Presumably, cranial similarities and differences among species reflect not just phylogenetic affinities, but also functional considerations. As Gans (1960) explained, the form of the facial skeleton in amphisbaenians may be influenced by different substrate types, different feeding modes, the loss or reduction of the eyes, and other functional and developmental forces. The "shovel-headed" *Rhineura floridana* burrows by driving its head down to penetrate the soil with its snout, then lifting it up to compress loosened soil particles onto the top of its burrow (Gans, 1974). The "round-headed" *Amphisbaena* is less obligately fossorial, and is considered to be a generalized burrower that forces its head through the soil in repeated forward pushes (Gans, 1974). The "spade-headed" *Diplometopon* burrows in much looser aeolian sands, using an oscillatory movement in which the head is rotated about the long axis of the body in alternate directions, thereby loosening soil from the tunnel walls as it progresses forward (Gans, 1974). The forces exerted on the skull during this type of burrowing are doubtless quite different from those exerted on the skulls of *Amphisbaena* or *Rhineura*, and this may explain the absence of extensive overlap of elements and interlocking sutures in *Diplometopon*.

It remains unclear the degree to which groupings of "round-headed," "shovel-headed," "spade-headed," and "keel-headed" forms reflect functional versus historical influences (Gans, 1978; Kearney, 2003). A recent molecular phylogenetic analysis offered evidence that limb reduction and loss has occurred more than once in amphisbaenian history (Kearney and Stuart, 2004). It also implied, as have virtually all previous analyses, that convergent evolution affected the head skeleton as well, but it is far more difficult at present to ascertain which particular cranial features are convergent. For example, if the molecular tree (Kearney and Stuart, 2004) proves more accurate than the morphological tree (Kearney, 2003), then many of the distinctions in facial architecture of the "spade-headed" *Diplometopon* may be transformations of relatively plesiomorphic conditions found in "shovel-headed" or "round-headed" forms. Although our present view of amphisbaenian phylogenetic history is incomplete, there is little doubt that convergent evolution has occurred throughout the skeleton. Until a stable phylogenetic hypothesis is recovered, it will be difficult to separate historical and functional influences. Toward this goal, ongoing detailed anatomical studies such as the present one will aid in the development of a more complete and accurate understanding of amphisbaenian cranial morphology.

ACKNOWLEDGMENTS

Scanning was performed by Richard Ketcham. We thank Olivier Rieppel and Kurt Schwenk for thoughtful reviews.

LITERATURE CITED

Bellairs Ad'A, Gans C. 1983. A reinterpretation of the amphisbaenian orbitosphenoid. Nature (Lond) 302:243–244.

Berman DS. 1976. A new amphisbaenian (Reptilia: Amphisbaenia) from the Oligocene-Miocene John Day Formation, Oregon. J Paleontol 50:165–174.

deBeer GR. 1937. The development of the vertebrate skull. Oxford: Oxford University Press.

El-Assy YS, Al-Nassar NA. 1976. Morphological study of the cranial osteology of the amphisbaenian *Diplometopon zarudnyi*. J Univ Kuwait (Sci) 3:113–141.

Estes R, de Queiroz K, Gauthier J. 1988. Phylogenetic relationships within Squamata. In: Estes R, Pregill G, editors. Phylogenetic relationships of the lizard families: essays commemorating Charles L. Camp. Stanford, CA: Stanford University Press. p 119–281.

Gans C. 1960. Studies on amphisbaenids (Amphisbaenia, Reptilia). 1. A taxonomic revision of the Trogonophinae and a functional interpretation of the amphisbaenid adaptive pattern. Bull Am Mus Nat Hist 119:129–204.

Gans C. 1974. Biomechanics. An approach to vertebrate biology. Philadelphia: JP Lippincott.

Gans C. 1978. The characteristics and affinities of the Amphisbaenia. Trans Zool Soc Lond 34:347–416.

Jollie MT. 1960. The head skeleton of the lizard. Acta Zool 41:1–64.

Kearney M. 2003. Systematics and evolution of the Amphisbaenia (Reptilia: Squamata) based on morphological evidence from fossil and living forms. Herp Monogr 17:1–75.

Kearney M, Stuart B. 2004. Repeated evolution of limblessness and digging heads revealed by DNA from old bones. Proc R Soc Lond 271:1677–1683.

Kearney M, Maisano JA, Rowe T. 2005. Cranial anatomy of the extinct amphisbaenian *Rhineura hatcherii* (Squamata, Amphisbaenia) based on high-resolution x-ray computed tomography. J Morphol 264:1–33.

Kesteven L. 1957. Notes on the skull and cephalic muscles of the Amphisbaenia. Proc Linn Soc New South Wales 82:109–116.

Kritzinger CC. 1946. The cranial anatomy and kinesis of the South African amphisbaenid *Monopeltis capensis* Smith. S Afr J Sci 42:175–204.

Lakjer T. 1927. Studien über die Gaumenregion bei Sauriern im Vergleich mit Anamniern und primitiven Sauropsiden. Zool Jahrb (Anat) 49:57–356.

Montero R, Gans C. 1999. The head skeleton of *Amphisbaena alba* Linnaeus. Ann Carn Mus 68:15–80.

Montero R, Gans C, Lions M. 1999. Embryonic development of the skeleton of *Amphisbaena darwini heterozonata* (Squamata: Amphisbaenidae). J Morphol 239:1–25.

Oelrich TM. 1956. The anatomy of the head of *Ctenosaura pectinata* (Iguanidae). Misc Publ Mus Zool Univ Mich 94:1–122.

Schwenk K. 2000. Feeding in lepidosaurs. In: Schwenk K, editor. Feeding: form, function and evolution in tetrapod vertebrates. San Diego, CA: Academic Press. p 175–291.

Vanzolini PE. 1951. Evolution, adaptation and distribution of the amphisbaenid lizards (Sauria: Amphisbaenidae). Ph.D. Thesis, Harvard University, Cambridge, MA.

Zangerl R. 1944. Contributions to the osteology of the skull of the Amphisbaenidae. Am Mid Nat 31:417–454.